

Photolysis of an Intrachain Peptide Disulfide Bond: Primary and Secondary Processes, Formation of H₂S, and Hydrogen Transfer Reactions

Olivier Mozziconacci,[†] Bruce A. Kerwin,[‡] and Christian Schöneich^{*,†}

Department of Pharmaceutical Chemistry, University of Kansas, 2095 Constant Avenue, Lawrence, Kansas 66047, and Department of Process and Product Development, Amgen Inc., 1201 Amgen Court West, Seattle, Washington 98119

Received: November 12, 2009; Revised Manuscript Received: January 23, 2010

The photodissociation of intrachain disulfide bonds in a model peptide and salmon calcitonin generates a series of cyclic peptide products following the generation of a CysS[•] thiyl radical pair. Key to the formation of these cyclic products are disproportionation and reversible hydrogen atom transfer reactions as well as secondary photoreactions, which lead to C–S bond breakage of primary photoproducts. Depending on the wavelength of the incident light, disulfides ultimately convert into cyclic thioethers. An important photolytic product is H₂S, which is highly relevant for the production and storage of protein pharmaceuticals, where H₂S can catalyze disulfide scrambling and protein degradation.

1. Introduction

The characterization of radical reactions following the photodissociation of a protein disulfide bond is an important aspect for understanding and preventing the formation of unwanted degradation products during the production and storage of proteins by the biotechnology industry. For example, antibodies contain multiple disulfide bonds, and, similar to many other proteins, are sensitive to light-induced degradation.^{1–3} The photodissociation of peptide disulfide bonds with 254 nm light leads predominantly to peptide cysteine thiyl radicals (CysS[•]).^{4,5} Ultimately, these may lead to protein aggregation and fragmentation, two phenomena that are frequently observed during antibody production and formulation.^{6–8} Moreover, these mechanisms may provide one chemical basis for adverse effects such as a potential of increased immunogenicity or loss of efficiency of antibody products. In addition, CysS[•] is a radical of special interest to biology and medicine. First, CysS[•] represents an important intermediate during catalytic turnover of several enzymes, such as, e.g., the ribonucleotide reductases.⁹ Second, CysS[•] engages in a variety of biologically relevant redox,^{10–13} addition,^{12,14,15} and abstraction^{16–20} reactions. In the present paper, we characterized several additional reactions originating from CysS[•] radicals in polypeptides specifically when generated through photolysis of an intrachain disulfide bond. These reactions, predominantly yielding cyclization products, are quite similar to analogous processes previously characterized for the photolysis of a cyclic organic disulfide, 4,5-dihydroxy-1,2-dithiane.²¹ The important features of these reactions are disproportionation and hydrogen transfer processes and secondary photoreactions of primary photoproducts.

CysS[•] can be formed as a result of disulfide photolysis, the one-electron oxidation of Cys,^{22–24} or the one-electron reduction of disulfide bonds.^{25,26} Specifically in proteins, the photoionization of protein Trp (or Tyr) residues can generate electrons, which subsequently reduce nearby protein disulfide bonds, as exemplified in a series of mechanistic studies on cutinase,^{27,28}

bovine growth hormone,²⁹ and α -lactalbumin.^{30,31} In α -lactalbumin, CysS[•] radicals are proposed to ultimately recombine with Trp-derived radicals to generate intraprotein cross-links, and for insulin a Cys–Tyr cross-link has been proposed.³² Experimental and theoretical data suggest that, within a protein, CysS[•] may be involved in a series of additional reactions with surrounding amino acids prior to recombination with CysS[•] or other radical intermediates.^{32–34} For example, theoretical calculations^{33,35,36} predict that within random peptide and β -sheet conformations, but not the α -helix, the ³C–H bond dissociation energy (BDE) of Gly is lower compared to the BDE of the S–H bond, resulting in a thermodynamic preference for hydrogen atom abstraction from Gly by CysS[•]. Previously, we had demonstrated quite efficient hydrogen abstraction reactions by CysS[•] when generated through photolysis of interchain disulfide bonds in model peptides and in insulin.^{32,37} Moreover, some evidence for the interaction of CysS[•] with the aromatic ring of Phe was provided.³⁸

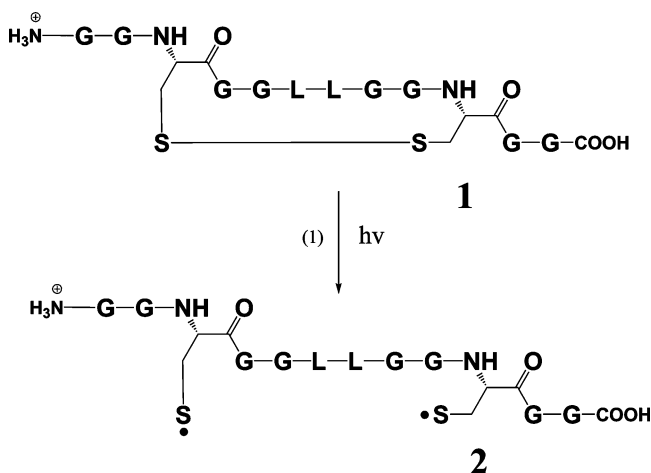
Theoretical studies by Thompson et al. suggest that the broad 250 nm absorption band of linear dialkyl disulfides contains two optical transitions.³⁹ Experimental studies indicate that the photolysis of dialkyl disulfides with wavelengths corresponding to their absorption maximum generates a singlet excited state through electronic $\sigma \rightarrow \sigma^*$ transition of the S–S bond,⁴⁰ resulting in the formation of predominantly a thiyl radical pair through homolytic S–S bond cleavage.^{4,41–43} While also C–S bond cleavage has been reported (predominantly for *tert*-butyl disulfide and penicillamine),^{44–46} our quantitative measurements for a disulfide-containing model peptide, glutathione disulfide, revealed >98% cleavage of the S–S bond into a thiyl radical pair.⁵ This is consistent with results of Kolano et al.,⁴⁷ who detected thiyl radicals during laser flash photolysis of intrachain disulfides of model peptides. Intersystem crossing (ISC) of thiyl radical pairs is very fast,⁴⁸ so that a large fraction of the initial singlet thiyl radical pair can be expected to convert into a triplet thiyl radical pair. This would explain our earlier results, where thiyl radicals generated by photodissociation of an interchain disulfide bond-containing model peptide produced significant yields of formal disproportionation products.^{32,37} Earlier photo-CIDNP studies have demonstrated such a disproportionation

* To whom correspondence should be addressed. Fax: (785) 864-5736. E-mail: schoneic@ku.edu.

[†] Department of Pharmaceutical Chemistry.

[‡] Department of Process and Product Development.

SCHEME 1: Photolysis at 253.7 nm of Peptide 1



mechanism for triplet radical pairs generated from the C–S cleavage of *tert*-butyl disulfide, but, interestingly, failed to detect polarized products from the photolysis of cystine.⁴⁴ However, the latter was ascribed to low quantum yields.

Here, we report on CysS[•] radical reactions generated from intrachain disulfide bonds, i.e., conditions which prevent separation of the initial CysS[•] radical pairs through diffusion. For most experiments, peptide thiyl radicals were generated through 253.7 nm photolysis of an intrachain disulfide in a short model peptide (**1**, Scheme 1) and in salmon calcitonin (sCT, Chart 1). In addition, photolysis at higher wavelengths up to 300 nm was carried out. We will provide evidence for a disproportionation mechanism, ultimately yielding a cyclic dithiohemiacetal (an α -mercapto-substituted thioether), which represents the origin for secondary photoproducts including thioethers, trisulfides, and H₂S. In addition, we will demonstrate the role of H₂S in the formation of the final photoproducts. In addition to its catalytic role for protein degradation, H₂S is emerging as an endogenously generated species with various functions in the nervous system, and pathological conditions, such as inflammation and cerebral ischemia. Various enzymes are implicated in H₂S formation in the brain and the vascular system.^{49–52} However, the biological activity of H₂S remains uncertain. Thus, the knowledge of potential sources of H₂S is important in view of the intriguing role that sulfhydryl radicals might play as a damaging or signaling species in the context of biological damage.

2. Experimental Section

2.1. Materials. A peptide containing an intrachain disulfide bond (GGCGLLGGCGG, **1**) was supplied by Amgen Inc. A similar peptide to **1** containing two additional arginine (Arg; R) residues (GGCRGLLGGRCGG, **1R**) was synthesized by the Biochemical Resource Service Laboratory (BRSL) at the University of Kansas, and purified to a purity level of >95%. Salmon calcitonin (sCT, Chart 1) was supplied by Bachem (Torrance, CA, USA). Sodium disulfide (Na₂S) and dithiothreitol (DTT) were supplied by Sigma-Aldrich (Saint Louis, MO). Pepsin, trypsin (sequencing grade), and endoproteinase Glu-C (sequencing grade) were supplied by Sigma-Aldrich (Saint Louis, MO), Promega (Madison, WI), and Roche (Nutley, NJ), respectively. *N*-Ethylmaleimide (NEM) and ThioGlo_1 (10-(2,5-dihydro-2,5-dioxo-1*H*-pyrrol-1-yl)-9-methoxy-3-oxo-, methyl ester-3*H*-naphthol[2,1-*b*]pyran-*s*-carboxylic acid) were supplied by Sigma-Aldrich (Saint Louis, MO) and Calbiochem (EMD Chemicals Inc., Gibbstown, NJ), respectively. Deuterium oxide (99.9% purity) was supplied by Cambridge Isotope Laboratories

(Andover, MA). These products were used without further purification. The digestion buffer consisted of 0.025 μ M of proteolytic enzyme and 20 μ M of either control, irradiated Arg-containing peptide (GGCRGLLGGRCGG) or irradiated sCT in the presence of citric acid buffer (pH 2.2, 50 mM) for peptic digestion, and ammonium bicarbonate buffer (pH 7.8, 50 mM) for either tryptic digestion or Glu-C digestion. Argon (Ar) at technical grade was used to saturate the solutions when necessary. NMR predictions were performed using the NMR tool implemented in ChemBioOffice 2008 (Cambridgesoft, Cambridge, MA).

2.2. UV Irradiations. The extinction coefficients of peptide **1** (1 mM) at 254 and 280 nm are 422 and 177 M^{−1} cm^{−1}, respectively. The extinction coefficients of peptide **1R** (1 mM) at 254 and 280 nm are 474 and 270 M^{−1} cm^{−1}, respectively.

2.2.1. UV Irradiation at $\lambda = 253.7$ nm. Peptides **1** and **1R** were dissolved in 400 μ L of H₂O (Milli-Q) or deuterium oxide at a 400 μ M concentration and the solutions saturated with Ar in quartz tubes prior to UV irradiation. sCT was dissolved in 1 mL of H₂O (Milli-Q) or in deuterium oxide at a concentration of 100–200 μ M and an aliquot of 200 μ L was placed in quartz tubes saturated with Ar. The samples containing **1** and **1R** were irradiated between 0 and 50 min, whereas the samples containing sCT were irradiated for 10 min. The irradiations were performed by means of four UV lamps emitting at 253.7 nm (Southern England, RMA-500).

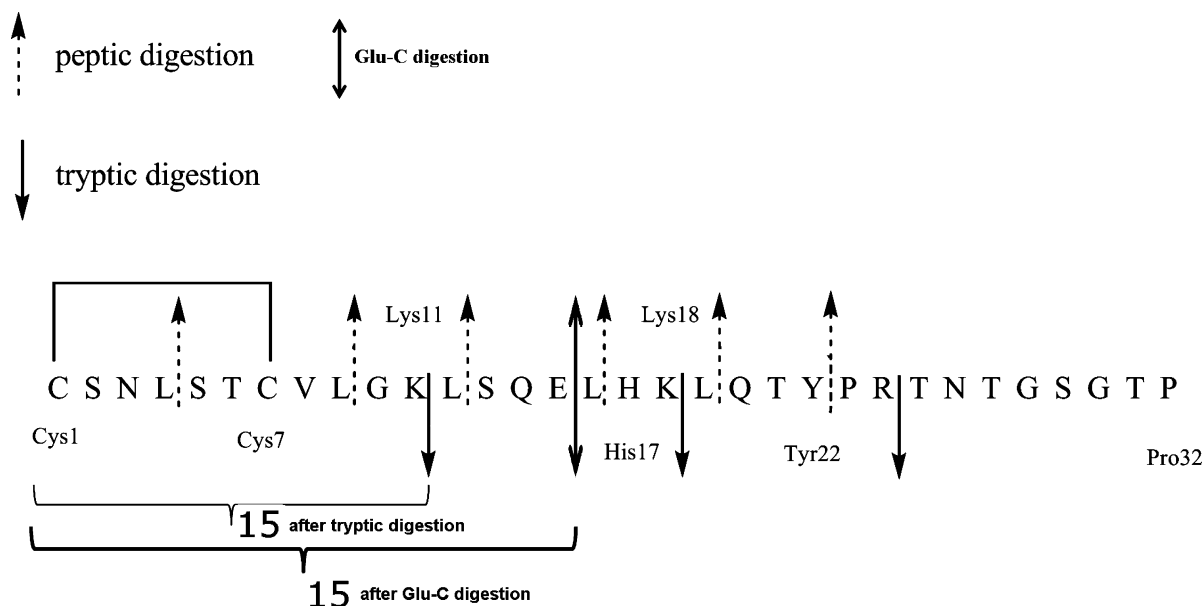
2.2.2. UV Irradiation at $\lambda = 280$ nm. UV irradiation of Ar-saturated solutions at 280 nm with a band-pass of 2 nm was performed with an arc lamp (Model 68806; Oriel Instrument) using an integrating sphere (Labsphere, Inc., North Sutton, NH), coupled to a monochromator (Model 77250; Oriel Instruments). The device is described elsewhere.²¹ Peptide **1** was dissolved in 1 mL of H₂O at a 400 μ M concentration and the solution saturated with Ar in a quartz cuvette that had been designed to fit the integrating sphere. The lower intensity of incident light, using the integrating sphere, necessitated irradiation of up to 9 h.

2.2.3. UV Irradiation with a Broader Spectrum of Light with $\lambda_{\text{max}} = 300$ nm. A few photoirradiation experiments were performed in a Rayonet reactor equipped with RPR-3000 Å lamps, for which the spectral distribution is centered at 300 nm and for which 93% of the photons emitted are in the wavelength range between 280 and 320 nm. Irradiations were either carried out in quartz or in Pyrex tubes.

2.3. UPLC-MS Analysis. The photoirradiated samples were injected onto a Vydac column (25 cm \times 1 mm C18, 3.5 μ m) and eluted with a linear gradient delivered at a flow rate of 90 μ L min^{−1} by an Acquity Ultra-Performance Liquid Chromatography system (Waters Corporation, Milford, MA). Mobile phases consisted of water/acetonitrile/formic acid at a ratio of 99%, 1%, and 0.08% (v:v:v) for solvent A and a ratio of 1%, 99%, and 0.06% (v:v:v) for solvent B. The following elution conditions were set: 1% of solvent B for 1 min, followed by a linear increase of B from 10 to 70% within 30 min.

2.4. Nano-Electrospray Ionization Time-of-Flight (ESI-TOF MS) Analysis. ESI spectra were acquired on a Q-TOF-2 (Micromass Ltd., Manchester, UK) hybrid mass spectrometer operated in the MS¹ mode and acquiring data with the time-of-flight analyzer. The instrument was operated for maximum resolution with all lenses optimized on the [M + 2H]²⁺ ion from the cyclic peptide gramicidin S. The cone voltage was 30 eV and Ar was admitted to the collision cell at a pressure that attenuates the beam to about 20% and the cell was operated at 5 eV (maximum transmission). Spectra were acquired at 11 364

CHART 1: Representation of Salmon Calcitonin (sCT) and the Respective Enzymatic Digestion Sites



Hz pusher frequency covering the mass range 100–2000 amu and accumulating data for 5 s per cycle. Time to mass calibration was made with CsI cluster ions acquired under the same conditions.

2.5. MS/MS Analysis. Collision-induced dissociation (CID) spectra were acquired by setting the MS¹ quadrupole to transmit a precursor mass window of ± 1.5 amu centered on the most abundant isotopomer. Ar was the collision gas admitted at a density that attenuates the beam to 20%; this corresponds to 16 psi on the supply regulator or 5.3×10^{-5} mbar on a penning gauge near the collision cell. MS/MS spectra were acquired with four different collision energies (22, 35, 45, 55 eV).

2.6. NMR Analysis. NMR spectra were acquired on a 500 MHz Bruker Avance spectrometer. Solvent signal suppression was achieved by transmitter presaturation. ¹H, COSY (correlation spectroscopy) measurements were performed in D₂O.

2.7. Covalent H/D Exchange and Isotopic Correction. The deuterium composition of peptide ions and their fragments was determined from the differences between the average mass of a covalently deuterated peptide and the average mass of the corresponding fully protonated peptide. The average masses were calculated from centroided isotopic distributions. The distribution of deuterium incorporation was obtained after isotopic correction by subtracting the isotope abundance distribution in the product formed during UV irradiation in H₂O from the isotope abundance distribution of the same product generated in D₂O. This variation of the isotopic distribution between the experiments performed in D₂O and H₂O will be given along this paper by the variation of the percent base peak intensity (%ΔBPI). A general mechanism illustrating the covalent H/D exchange is presented in Scheme 2. The derivatization of the available thiol group with *N*-ethylmaleimide (NEM) is required to chromatographically separate the photoproducts. The reaction of thiolate with the carbon–carbon double bond of NEM in D₂O leads to deuterium incorporation into the derivatized photoproduct. Thus, chemical derivatization of the photoproducts was performed in solutions containing an equal amount of H₂O and D₂O (1:1, v:v). [After UV irradiation the H₂O (or D₂O) samples were diluted with an equal volume of D₂O (or H₂O), respectively.] Consequently, only the photochemical mechanisms, involving covalent deuterium incorpora-

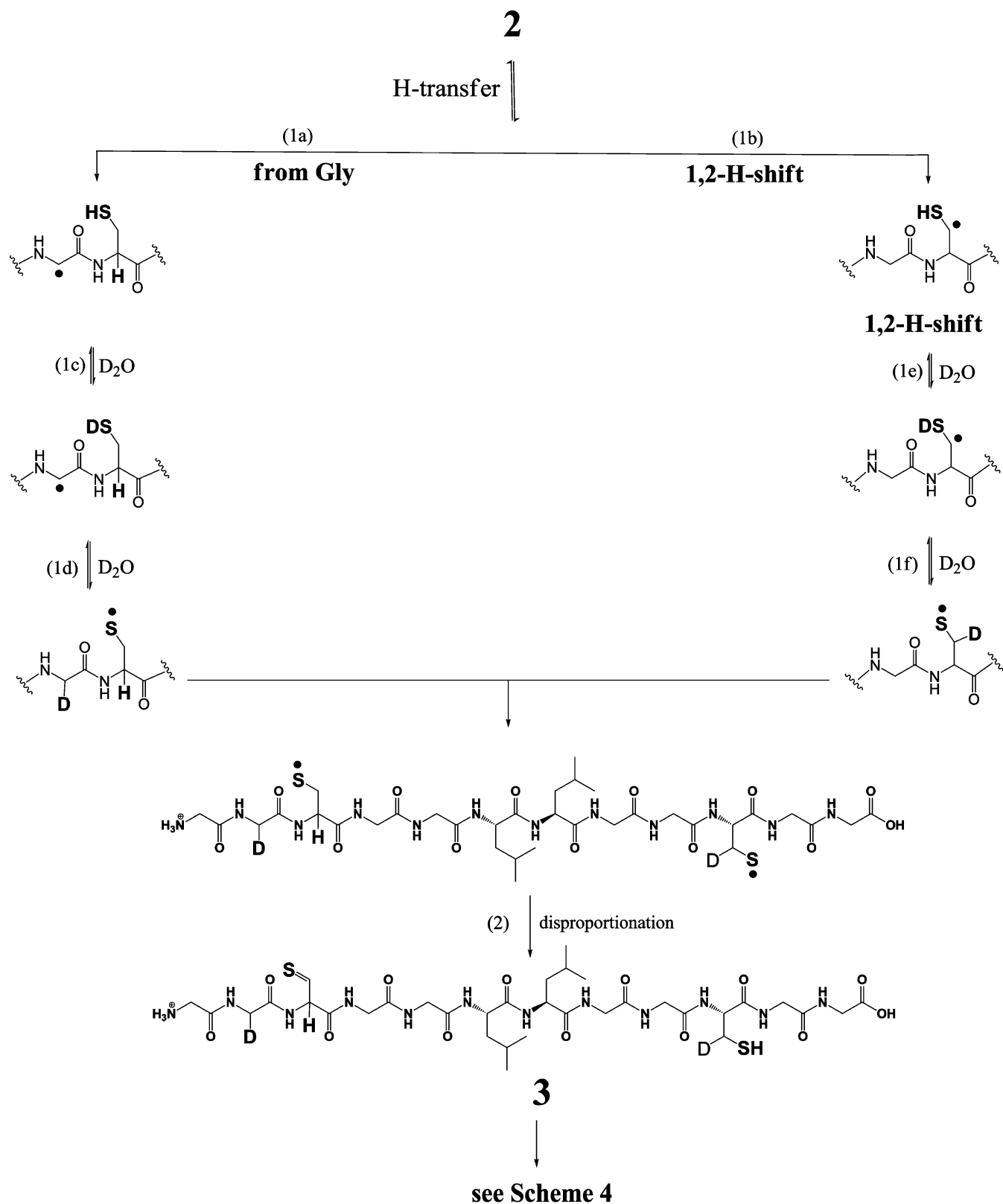
tion during the formation of the photoproducts, will be indicated by a difference of deuterium incorporation analyzed by MS.

The number of deuterium atoms incorporated into the photoproduct was approximated as follows: a linear combination of seven different isotopic distributions was performed. The isotopic distributions consisted of seven different isotopic distributions of the photoproduct. The first isotopic distribution was the experimental one obtained after formation of the photoproduct in H₂O. The six other isotopic distributions were the theoretical isotopic distributions obtained in the case where 100% of the molecules of the photoproduct would have incorporated one to six deuterium atoms. The coefficients of the linear combination were obtained for the best fit of the simulation with the experimental isotopic distribution of the photoproduct produced in D₂O. After normalization of the sum of the coefficients to 1, we could estimate the ratio of molecules of the photoproduct which incorporated 0 to 6 deuterium atoms. An example of this simulation is given in the Supporting Information.

2.8. Detection of Volatile Mercaptans. Volatile mercaptans, generated during UV irradiation of an aqueous Ar-saturated solution containing peptide **1**, were continuously transferred from the irradiated solution (Supporting Material, Chart S1, vial 1) using Ar as a carrier gas, and trapped in a second vial (Supporting Material, Chart S1, vial 2) containing either a 5 mL solution of ThioGlo_1 reagent for fluorescence analysis^{53,54} or NEM, adjusted to pH 7.5 using concentrated NaOH (1 M), and protected from light by several layers of alumina foil.

2.8.1. Fluorescence Detection. ThioGlo_1 fluoresces with high quantum yields ($\Phi = 0.49$) after reaction with RSH/RS[−], exhibiting only an extremely low baseline fluorescence.⁵⁴ The time course for fluorescence development between ThioGlo_1 and RS[−] in vial 2 (Supporting Material, Chart S1) was monitored over 50 min by taking representative aliquots, analyzed on a spectrofluorophotometer (Shimadzu, RF 5000U) with the excitation and emission wavelengths set at 379 and 513 nm, respectively.⁵³

2.8.2. Mass Spectrometry Analysis. The ThioGlo_1 reagent solution in vial 2 (Supporting Material, Chart S1) was replaced by NEM. Although Q-TOF mass spectrometry analysis is a sensitive analytical tool, its sensitivity is much lower than

SCHEME 2: Reaction Scheme for Covalent H/D Exchange^a

^a The intramolecular H-atom transfer occurs between the thiyl radical of the cysteine residue and ^αC–H and/or ^βC–H.

fluorescence detection. Thus, in order to identify the structure of the products resulting from the derivatization of the maleimide function of NEM with RS[−], the volatile mercaptanes were collected during 90 min of UV irradiation of the solution containing peptide **1**. Then, an aliquot of the NEM solution was analyzed by UPLC-MS.

2.9. Quantum Yield. The quantum yield (Φ) was calculated using the integrating sphere (as described above, section 2.2.2) and according to eq I. Here P_{abs} refers to the amount (in mole) of photons absorbed, P_{c} to the amount of photons reflected from a control sample lacking peptide **1**, and P_{s} to the amount of photons reflected from a sample containing peptide **1**. P_{abs} was

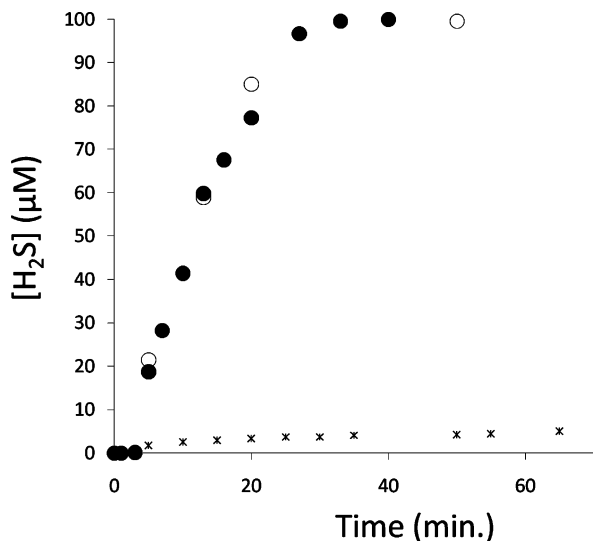


Figure 1. Time course of the fluorescence development in a 100 μM (●, ○) ThioGlo_1 solution used to trap H_2S . The fluorescence is due to the reaction of the maleimide group of ThioGlo_1 with H_2S (Scheme 3). H_2S was generated by UV irradiation at 253.7 nm of a solution containing peptide 1 (400 μM) at pH 7.2 (●) or pH 3.4 (○). At both pH values, photoirradiation of peptide 1 in a Rayonet reactor equipped with UV lamps, of which the spectral distribution is centered at 300 nm and for which 93% of the photons emitted are in the wavelength range between 280 and 320 nm, does not yield H_2S (*).

calculated according to eq II. The Q-TOF instrument was calibrated using a specific amount (in mole) of peptide 1. Thus, the moles of product produced were calculated from the absolute intensity given by the Q-TOF after LC-MS analysis.

$$\Phi = \text{mole of product} / P_{\text{abs}} \quad (\text{I})$$

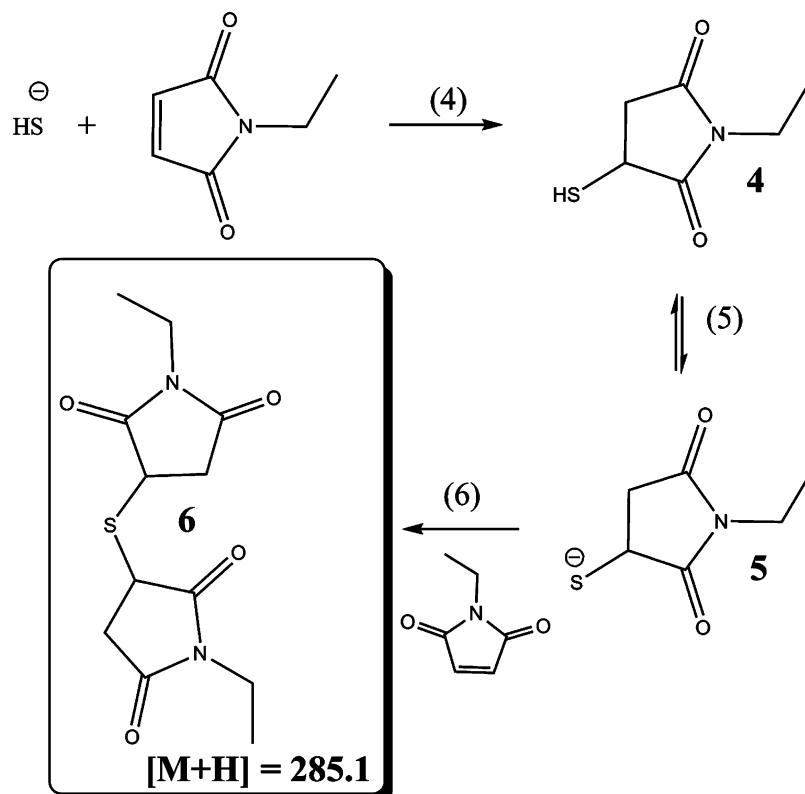
$$P_{\text{abs}} = P_{\text{c}} - P_{\text{s}} \quad (\text{II})$$

3. Results

3.1. UV Irradiation of Peptide 1. 3.1.1. Detection of H_2S .

UV Irradiation at 253.7 nm. (i) Fluorescence Detection. Ar-saturated aqueous solutions of peptide 1 at pH 3.4 or pH 7.2 were irradiated up to 50 min. In a first experiment, volatile reaction products were transferred from vial 1 into vial 2, which contained 100 μM ThioGlo_1 at pH 7.5 (Supporting Material, Chart S1). To ensure the complete resolubilization of the volatile components, the carrier gas was transferred through a needle with the outlet placed at the bottom of a 5 mL solution (depth $\approx 5\text{--}6$ cm). To measure the time course of the fluorescence increase of the ThioGlo_1 solution during the irradiation, an aliquot of 1 mL was periodically taken from the ThioGlo_1 solution for analysis (Supporting Material, Chart S1, vial 2). The results for acidic and neutral solutions are presented in Figure 1. To quantify the amount of H_2S formed during the irradiation, the spectrofluorimeter was calibrated using different concentrations of Na_2S . The evolution of the concentration of H_2S for both irradiation conditions (pH 3.4 and pH 7.2) is similar. After a short lag period (0–2 min), due, in part, to the equilibration of H_2S between solution and headspace in vial 1, the intensities of the fluorescence increased nearly linearly for a period of ca. 20 min to reach a plateau after ca. 28 min (100 μM). The height of the plateau depends on the ThioGlo_1 concentration available for reaction. The presence of a volatile mercaptane suggests the formation of H_2S . At neutral pH, H_2S deprotonates to HS^- (eq 1, $\text{pK}_{\text{a}} = 6.9$)⁵⁵ which reacts efficiently with ThioGlo_1. Importantly, after the reaction of HS^- with

SCHEME 3: Reaction Scheme for the Derivatization of H_2S with NEM



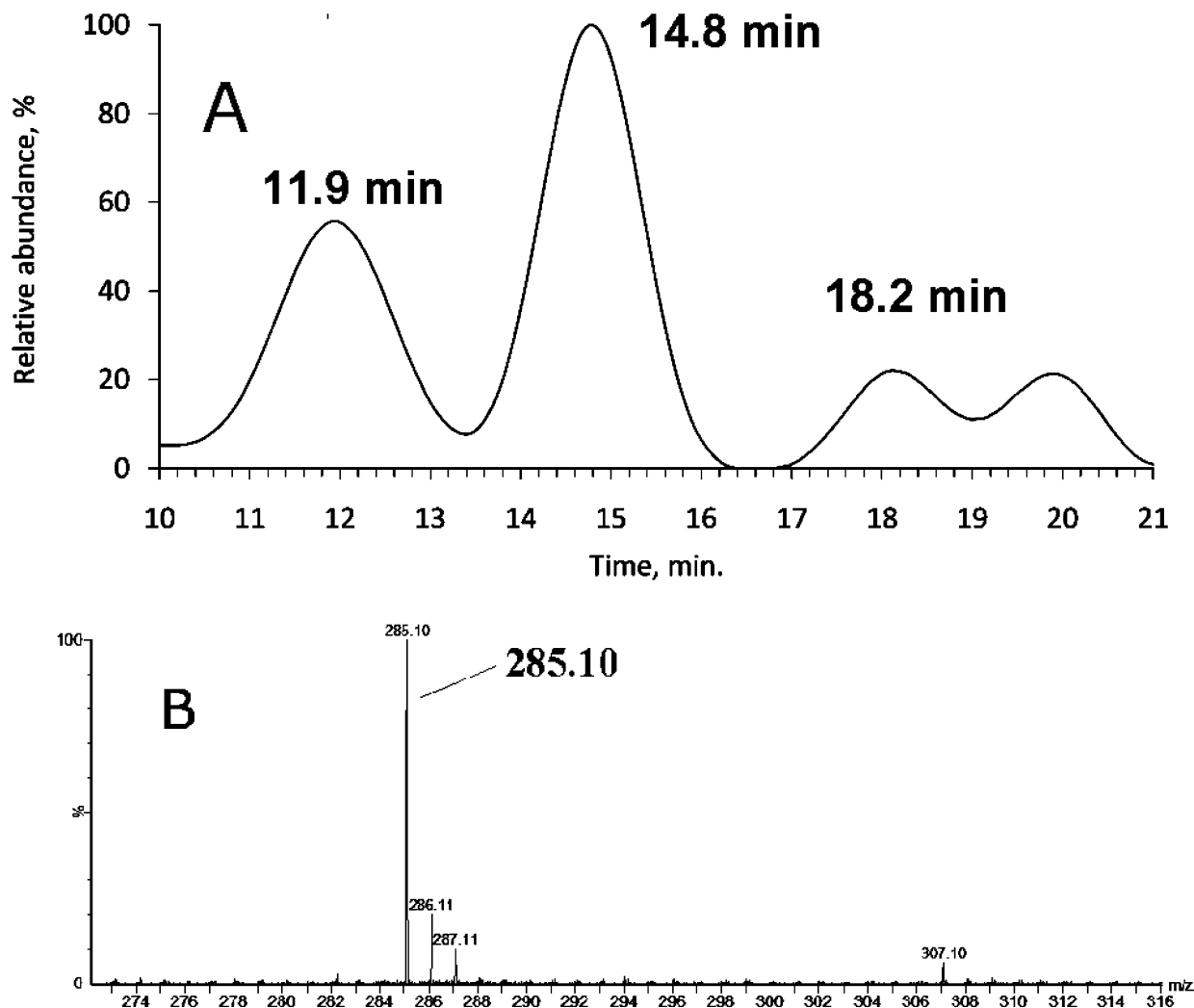


Figure 2. UPLC-MS analysis of NEM-containing aqueous solution (100 μ M) after trapping volatile mercaptans during 90 min of photoradiation. The volatile mercaptans were removed continuously from the irradiated sample using Ar as a carrier gas. The experimental protocol is presented in Chart S1 (Supporting Information). (A) Chromatography, and (B) MS spectrum of the peak eluting at 11.9 min.

the maleimide reagent, the product represents again a thiol, which should theoretically react with a second molecule of ThioGlo_1. Hence, we designed a mass spectrometry experiment to confirm the reaction of H_2S with two maleimide molecules.



(ii) *Mass Spectrometry Analysis.* Ar-saturated aqueous solutions containing peptide **1** (Supporting Information, Chart S1, vial 1) were irradiated over 90 min, and the gases collected in vial 2 containing NEM instead of ThioGlo_1 (Supporting Information, Chart S1, vial 2). After irradiation, the solutions in vials 1 and 2 were analyzed by mass spectrometry. The UPLC-MS data presented in Figure 2 display three peaks, eluting with $t_R = 11.9$, 14.8, and 18.2 min (Figure 2A). Product **6** (Scheme 3), with m/z 285.1 (Figure 2B), eluted after 11.9 min, and corresponds to the expected mass of one molecule of H_2S derivatized with two molecules of NEM (Scheme 3). The two other peaks (Figure 2, appearing at 14.8 and 18.2 min) represent H_2S derivatized with NEM, which had undergone hydrolysis of the maleimide function.

3.1.2. Analysis of Nonvolatile Photoproducts. Ar-saturated aqueous solutions containing peptide **1** were photolyzed at 253.7 nm (≤ 10 min) or 280 nm (9 h) at pH 7.2 and 3.4. The different

photolysis times were mandated by the different intensities emitted by the various light sources. Subsequently, the pH of the irradiated solutions was adjusted to pH 7.5 by addition of 1.0 M NaOH for derivatization with NEM. All potentially isobaric derivatized photoproducts were separated by UPLC. The stoichiometry of NEM incorporation into the photoproducts will indicate the number of thiol groups generated by photolysis. Here a shift in mass equal to a multiple of the mass of NEM (m/z 125.0) will quantify the number of free thiols in each photoproduct. The UPLC chromatograms obtained after derivatization of the photoproducts with NEM (Figure 3, (A) neutral solution, (B) acidic solution) reveal the formation of nine photoproducts with the following m/z : 873.4, 937.4, 998.4, 1014.4, 1030.4, 1062.4, 1155.4, 1157.4, and 1187.4. The tentative structures of these photoproducts are presented and framed in Schemes 4–7. Except for products **7-NEM** and **9**, for which additional NMR data were collected, all of the structural assignments are based on MS and MS/MS analysis prior and/or subsequent to derivatization with NEM.

(a) *Photoproducts Formed after UV Irradiation at 253.7 nm.* The tentative structures are presented in Table 1 and the tentative mechanisms for formation of the products are presented in Schemes 4–7. These mechanisms have been formulated based on mechanistic studies performed after a complete product

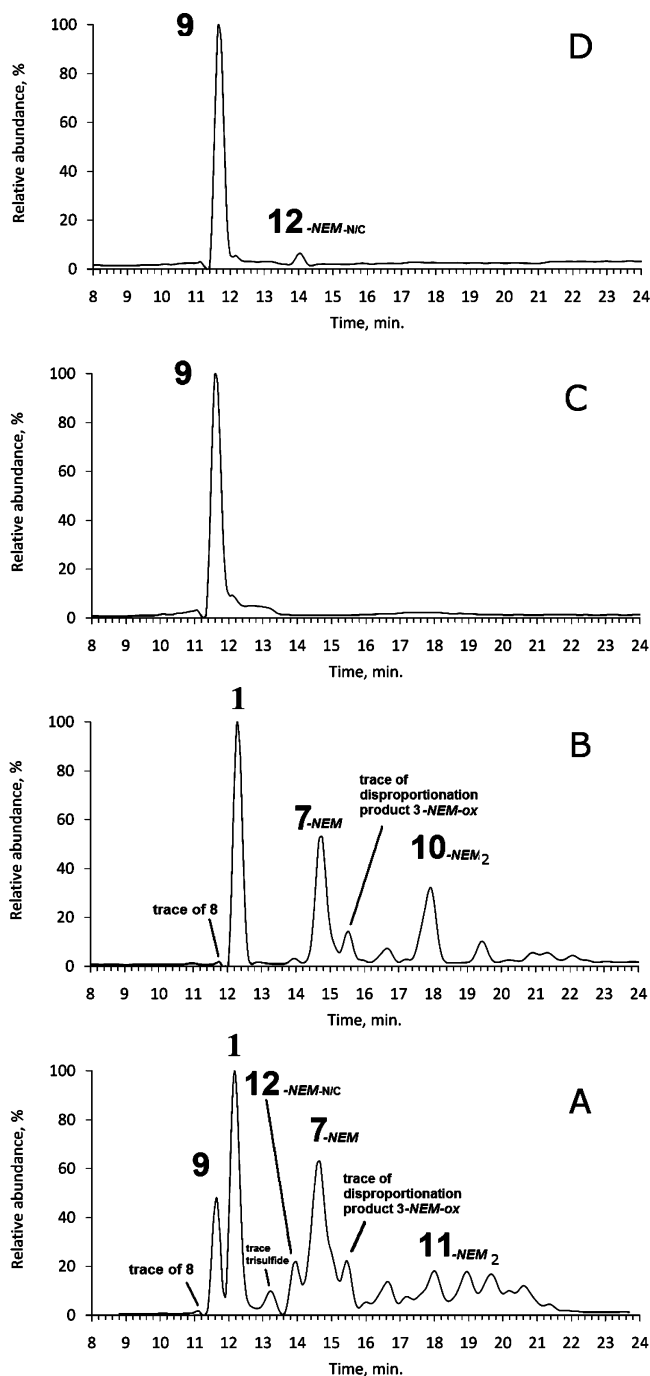


Figure 3. UPLC-MS chromatograms of the photoproducts generated after UV irradiation at 253.7 nm of **1** in Ar-saturated solution: (A) at pH 7.2, (B) at pH 3.4, (C) at pH 3.4 or pH 7.2 under continuous Ar-flow maintained during the irradiation to remove volatile products, and (D) derivatization with NEM of the solution analyzed by UPLC-MS and presented in chromatogram C.

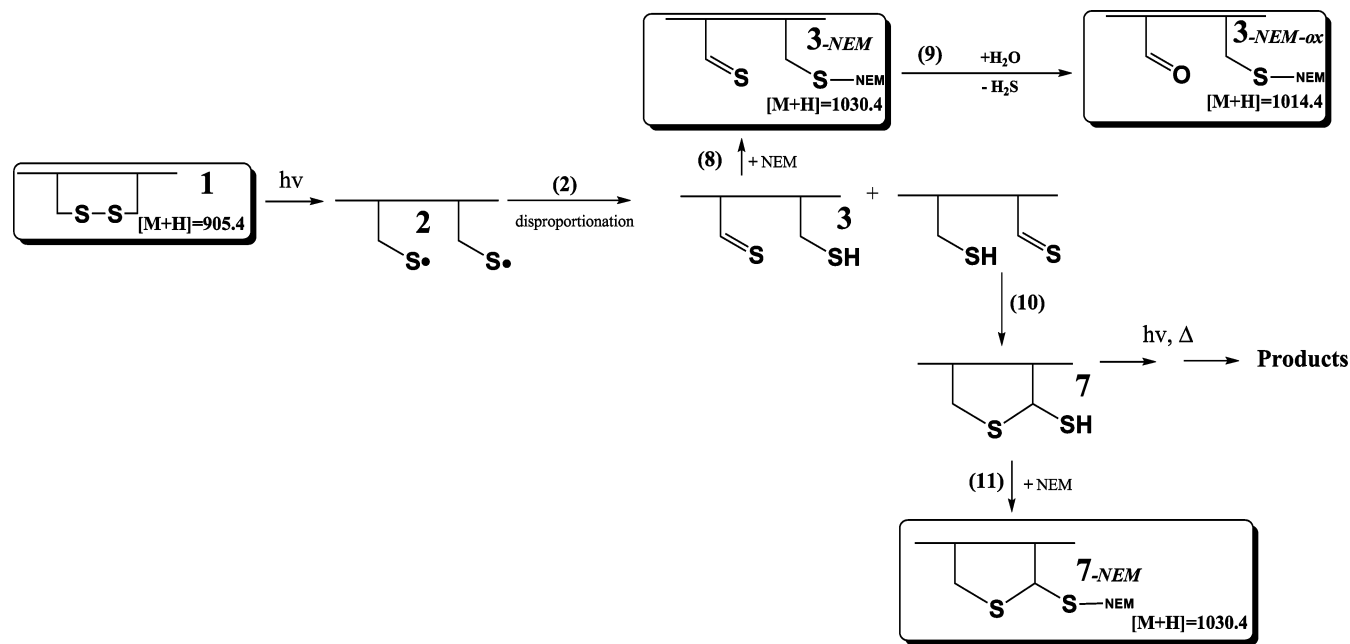
characterization. The mechanistic studies are presented in sections 3.1.3, 3.1.4, and 3.1.7.

(i) **Products 3 and 3-NEM-ox** ($m/z = 1014.4$). Product **3** (observed as **3-NEM-ox**, Scheme 4) is formed at both neutral and acidic pH and elutes after 15.2 min (Figure 3A,B). The low quantities of **3-NEM-ox** do not allow for a complete MS/MS sequencing. However, the MS/MS fragmentation yields three important fragments: y_7 , y_8 , and b_6 . These fragments confirm that **3-NEM-ox** is a linear peptide (Figure S1, Supporting Information). In addition, these fragments confirm that one Cys residue is derivatized with NEM; the thiol of the other Cys residue is transformed into aldehyde.

(ii) **Products 7 and 7-NEM** ($m/z = 1030.4$). Product **7** (observed as **7-NEM**, Scheme 4) is formed at both neutral and acidic pH and elutes after 14.7 min (Figure 3A,B). The difference of mass between product **7-NEM** and the native peptide **1** (m/z 905.4) is equal to the mass of NEM (125 amu; amu = atomic mass unit) which demonstrates the presence of one free thiol. A product isobaric to **7-NEM** is also observed with a retention time of $t_R = 15.4$ min. The MS/MS fragmentation of product **7-NEM** yields several important fragments: y_{10} , y_{11} , b_{10} , and b_{11} (Figure S2, Supporting Information). The absence of the other b and y fragments suggests the formation of a cyclic product involving both cysteine residues. Importantly, an analogous cyclization product was obtained during photoirradiation of an organic disulfide, 4,5-dihydroxy-1,2-dithiane.²¹ An internal fragment containing the cyclic structure “W” (Figure S2, Supporting Information) is consistent with intramolecular cyclization of the sequence CGLLGGC. Two other internal fragments showing the derivatization of the C-terminal Cys residue, LGGC-NEM and LLGGC-NEM, are also consistent with the structure of **7**. The heterolytic cleavage of the C–S bond, labeled (1), results in the formation of a positive ion with m/z 871.4. This fragment demonstrates the possible loss of ^-S -NEM during MS/MS fragmentation. The poor MS/MS data for the additional product isobaric to **7** ($t_R = 15.4$ min) do not allow any assignment of structure. Importantly, product **7** does not react with dithiothreitol (DTT). This result confirms the involvement of one of the sulfur atoms in an additional C–S bond. The α -mercapto-substituted cyclic thioether motif observed in product **7-NEM** was also formed after photoirradiation of the disulfide- and Arg-containing peptide (GGCRGLLGGRCGG), referred to as **7Ra-NEM** (Chart 2). Here, trypsin digestion allows to open the cyclic structure through proteolytic cleavage C-terminal of Arg (Chart 2, **7Rb-NEM**). Thus, the MS/MS fragments of each strand of the peptide (y_1 , y_3 , b_2 , a_3 , and b'_2) can confirm a cross-link between the cysteine residues and the presence of a thiol residue which is derivatized with NEM (Figure S3, Supporting Information). In addition, the heterolytic cleavage of the C–S bond, noted by (Δ), generates a positive ion (the positive and negative charges are held by the carbon and the sulfur atoms, respectively) with m/z 515.2 corresponding to the sequence GGCR where the thiol of the cysteine residue is derivatized with NEM. Interestingly, the difference of mass between this latter ion and the fragment denoted (Θ) with m/z 483.2 is equal to 32 Da. This observation suggests the loss of sulfur as part of a gas phase rearrangement. Moreover, the difference of mass between the fragment (Θ) with m/z 483.2 and the fragment (\wedge) with m/z 358.2 is equal to 125 Da, which corresponds to the mass of NEM. (The NMR analysis of **7-NEM** and **9**) will be described below.)

(iii) **Product 8** ($m/z = 871.4$). Product **8** (Scheme 5) is formed at both neutral and acidic pH and elutes after 11.2 min (Figure 3, A, B). Product **8** cannot be derivatized with NEM. The low amount of this product precludes a careful analysis by MS/MS fragmentation. However, the elution time of **8** is similar to that observed for product **9**, suggesting that **8** is structurally close to **9**. The location of the double bond is suggested by the proposed mechanism of formation and further reaction (see below).

(iv) **Product 9** ($m/z = 873.4$). Product **9** (Schemes 5 and 6) is generated exclusively in neutral solution. It elutes with $t_R = 11.7$ min (Figure 3A). The difference of mass between **9** and the native peptide **1** is 32 amu, suggesting the loss of sulfur. Product **9** cannot be derivatized with NEM, confirming the absence of free thiol residues. The MS/MS fragmentation of **9**

SCHEME 4: Reaction Scheme for the Formation of the Major Product 7 Formed after UV Irradiation ($\lambda > 280$ nm) of an Aqueous Ar-Saturated Solution Containing Peptide 1 at pH 3.4


displays the fragments b10, b11, y10, and y11 (Figure S4, Supporting Information). The absence of fragments b3–b9 and y3–y9 suggest the formation of a cyclic peptide involving both original cysteine residues. Here, mechanistically the loss of sulfur precedes the cyclization. An internal fragment denoted “Z” is consistent with the cyclic nature of product 9. An interesting internal fragment is observed with m/z 558.3. This fragment is rationalized by a rather unusual cleavage involving the fragmentation sites b3 and b10 and cleavage of the C–S bond (Figure S4 (Supporting Information), cleavage “(a)”). An analogous fragment was described by Datola et al.⁵⁶ for the MS analysis of a cyclic thioether peptide of human growth hormone. The cyclic-thioether motif observed in product 9Ra was also formed during the photoirradiation of the disulfide- and Arg-containing peptide (GGCRGGLLGRCGG, Chart 3). After tryptic digestion of the cyclic product peptide 9Ra, the MS/MS fragments of each strand of product 9Rb (y1, y3, b2, a3, and b'2) confirm a cross-link between the original cysteine residues (Chart 3, Figure S5, Supporting Information). In addition, the heterolytic cleavages of the C–S bonds (the positive and negative charges are held by the carbon and sulfur atoms, respectively), noted (Δ) and (\ominus), generate two fragments with m/z equal to 358.2 and 390.1, respectively. Interestingly, a fragment with m/z 358.2 was also observed after MS/MS fragmentation of the α -mercapto-cyclic-thioether (product 7Rb-NEM, Figure S3, Supporting Information). Hence, the ion with m/z 358.2 must result from the loss of sulfur and the loss of NEM after the fragmentation of the C–S bond (cleavage (Δ), Figure S3, Supporting Information). In the cyclic-thioether, 9Ra, the absence of a thiol residue allows directly the release of the ion with m/z 358.2 without any further rearrangement.

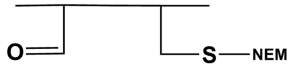

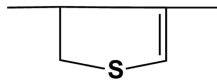
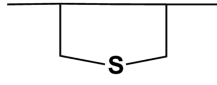

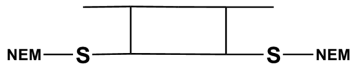


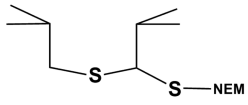
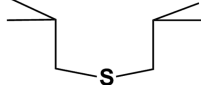
(v) Product 10 and 10-NEM₂ ($m/z = 1157.4$). Product 10 (observed as 10-NEM₂, Scheme 7) is exclusively formed in acidic solution. It elutes with $t_R = 18.1$ min (Figure 3A). The MS/MS fragmentation of 10-NEM₂ (Figure S6, Supporting Information) shows fragments b3–b7, b10, and y3–y9. These fragments demonstrate clearly that 10-NEM₂ is a linear peptide where both cysteine residues are derivatized with a molecule of NEM.

(vi) Product 11 and 11-NEM₂ ($m/z = 1155.4$). Product 11 (observed as 11-NEM₂, Scheme 5) is formed predominantly in neutral solution and elutes with $t_R = 17.9$ min (Figure 3B). The difference of mass between 11-NEM₂ and the native peptide 1 amounts to 250 amu, suggesting the presence of a second free thiol group in 11-NEM₂ (compared to 7-NEM), that can be derivatized with a second molecule of NEM. The MS/MS fragmentation of 11-NEM₂ (Figure S7, Supporting Information) reveals the fragments b10, b11 and an internal fragment referred to as “X”, where both cysteine residues are derivatized with NEM. In addition, we observe the internal fragments LGGC and LLGGC where the respective cysteines are derivatized with NEM (Figure S7, Supporting Information). This internal fragmentation pattern is consistent with the formation of a cyclic product, cross-linking between the carbon-atoms of both cysteine residues. Based on mechanistic considerations (a proposed 1,2-H-shift of the CysS' radicals; see below), we tentatively assign a cross-link between the Cys β C-atoms to product 11.

(vii) Products 12-N/C and 12-NEM-N/C ($m/z = 998.4$). Products 12-N/C (observed as 12-NEM-N/C, Scheme 6) are generated in neutral solution and show derivatization with NEM. They elute with $t_R = 14.0$ min (Figure 3A). The MS/MS fragmentation of 12-NEM-N (Figure 4) reveals elimination of H_2S from the C-terminal cysteine residue (Figure 4, fragments y7, y8) and the derivatization of the thiol group of the N-terminal cysteine residue with one molecule of NEM (Figure 4, fragments b5, b6, b7). The masses of fragments y7, y8, b10, and b11 are consistent with the conversion of one Cys residue into dehydroalanine. The observation of the fragments b'7 and y'8 is consistent with the presence of 12-NEM-C where the N-terminal cysteine is transformed into a dehydroalanine residue.

(viii) Products 13-N/C and 13-NEM-N/C ($m/z = 1000.3$). Products 13-N/C (observed as 13-NEM-N/C, Scheme 6) are formed in neutral solution after UV irradiation of peptide 1. Increased yields of 13-N/C are observed also after photoirradiation of product peptide 10 at neutral pH (see below). It elutes with $t_R = 14.8$ min (Figure S16B, Supporting Information). The MS/MS fragmentation of 13-NEM-C (Figure S9, Supporting Information) shows fragments a3/b3, b6, b7, b10, and y5–y9.

TABLE 1: Tentative Structures of the Products Observed after Photoirradiation ($\lambda = 253.7$ nm) and Derivatization with *N*-Ethylmaleimide (NEM) of the Peptides 1 and 1R

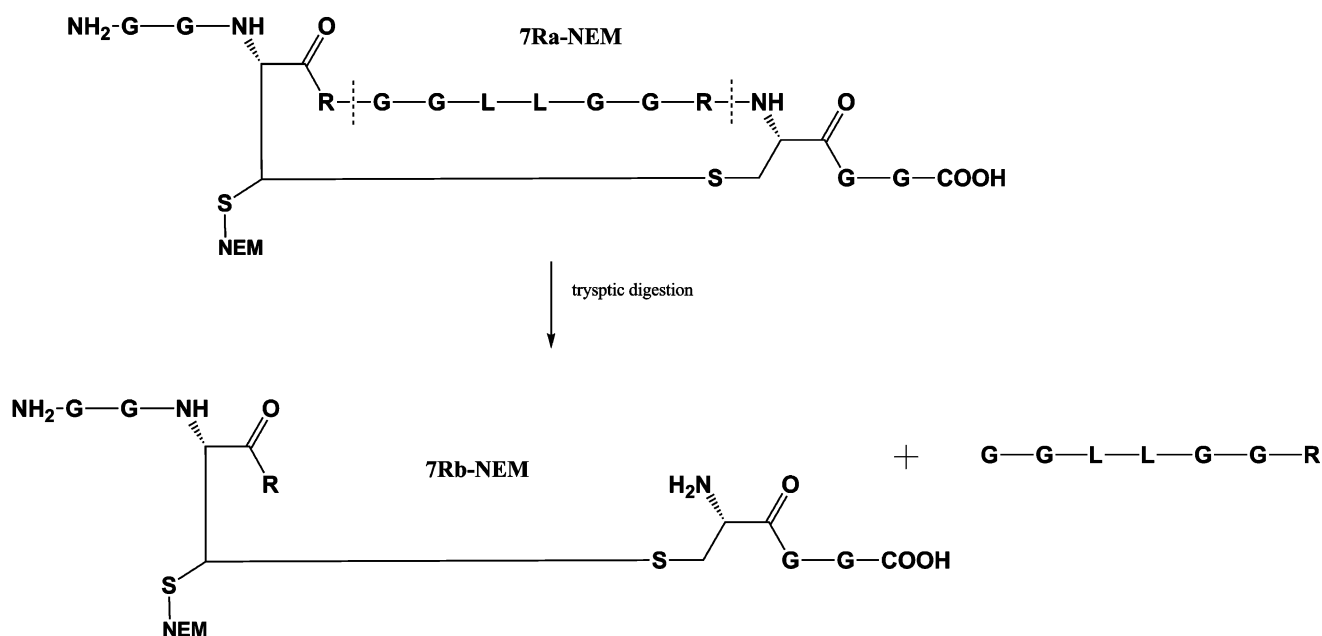
Name of the products	Tentative structures	Masses (m/z)
<i>Tentative structures of products obtained after photo-irradiation of peptide 1</i>		
3-NEM-ox		1014.4
7-NEM		1030.4
8		871.4
9		873.4
10-NEM ₂		1157.4
11-NEM ₂		1155.4
12-NEM-N/12-NEM-C		998.4
13-NEM-N/13-NEM-C		1003.3
<i>Tentative structures of products obtained after photo-irradiation of peptide 1R and tryptic digestion</i>		
7Rb		750.2
9Rb		593.2

These fragments demonstrate clearly that **13-NEM-C** is a linear peptide where the C-terminal cysteine residue is derivatized with a molecule of NEM whereas the N-terminal cysteine is formally transformed into an alanine residue. A few characteristic fragments (b'6, b'8, and b'9) are also observed for product **13-NEM-N**.

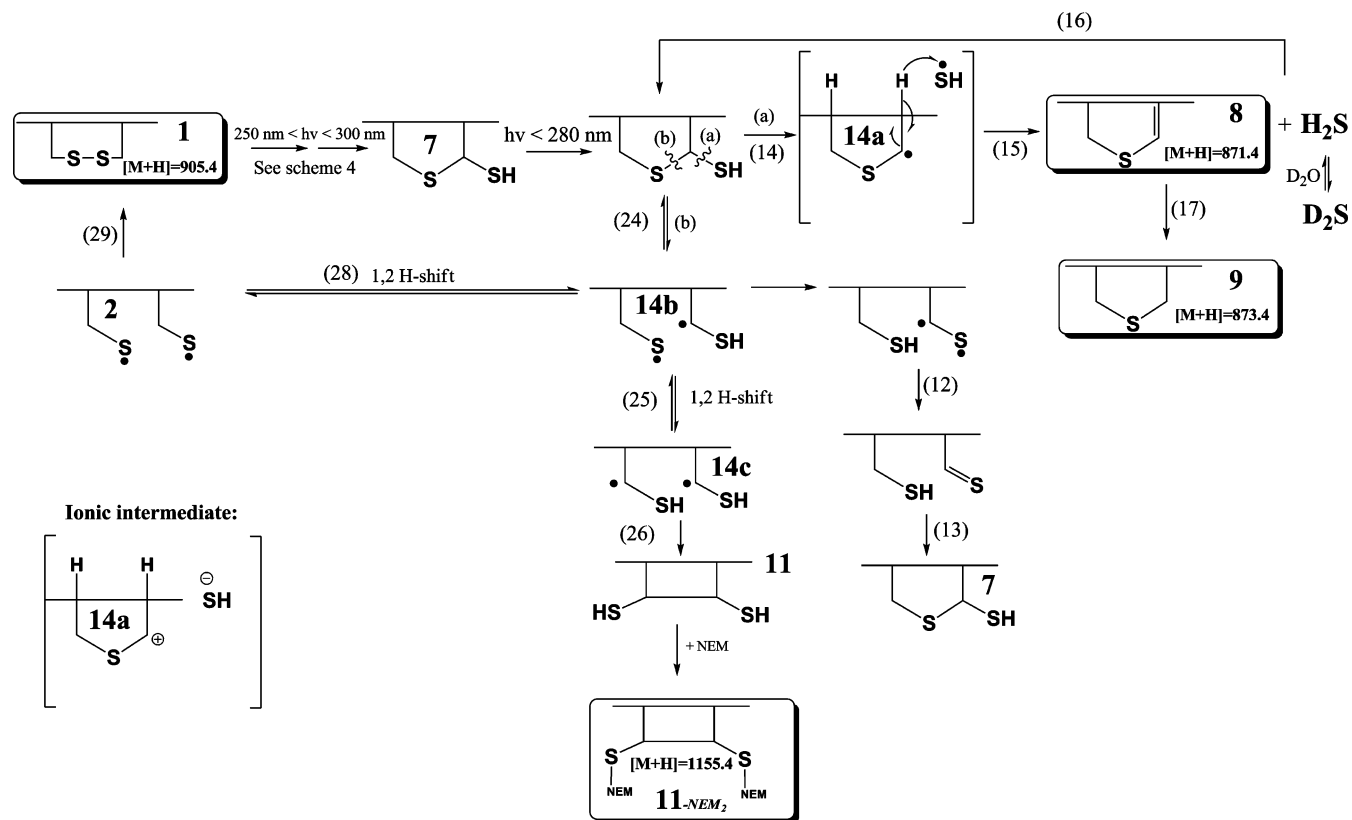
(ix) *Peptide Dimers*. After UV irradiation of peptide **1** at either pH 3.4 or 7.2 low yields of several dimers are observed. These products elute between $t_R = 18.5$ and 22.5 min (Figure 1A,B) and appear as doubly charged ions in the mass spectra. The m/z of these products corresponds to recombination products of the initial diradicals from peptide **1**.

CHART 2: Representation of Products 7Ra-NEM and 7Rb-NEM Obtained after Photolysis of the Peptide (GGCRGGLLGRCGG), NEM Derivatization, and Tryptic Digestion^a

tryptic digestion

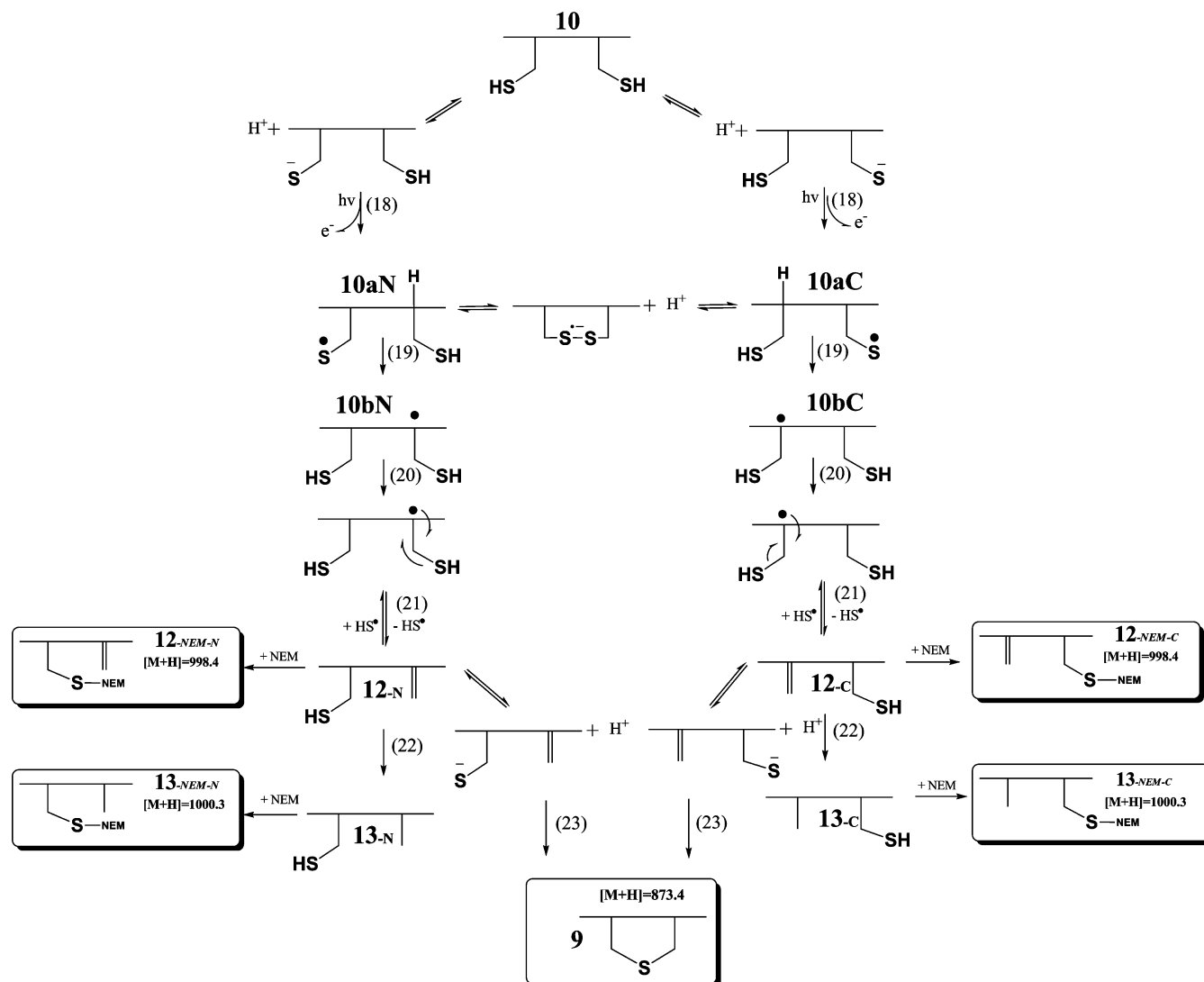
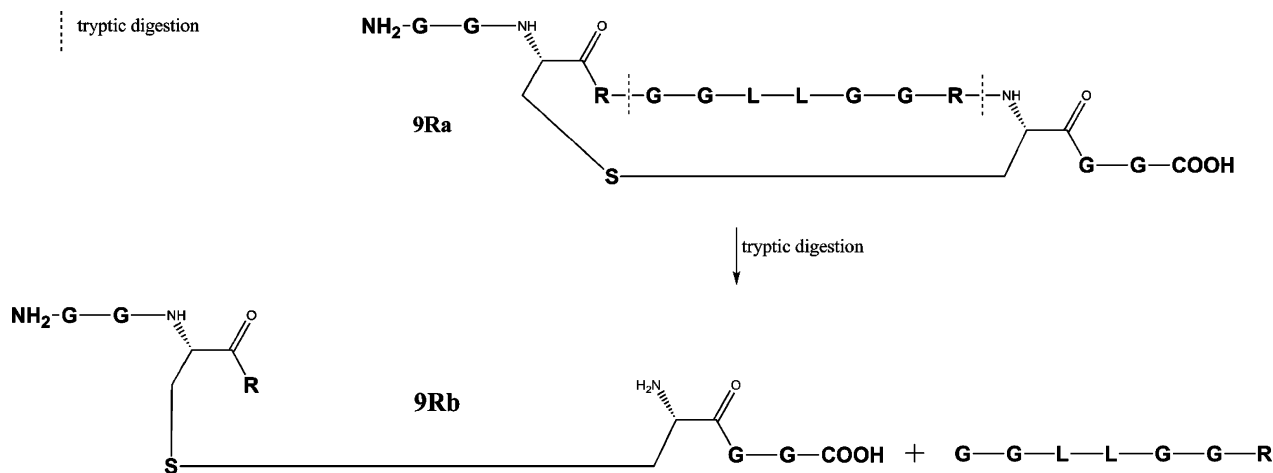


^a The tryptic digestion sites are indicated with the dashed lines. The photolysis was carried out in a Rayonet reactor equipped with UV lamps of which the spectral distribution is centered at 300 nm and for which 93% of the photons emitted are in the wavelength range between 280 and 320 nm.

SCHEME 5: Reaction Scheme of the Secondary Processes Occurring during the Photolysis of Peptide 1 after UV Irradiation ($\lambda = 253.7$ nm) of an Aqueous Ar-Saturated Solution

(b) Photoproducts Formed after UV Irradiation at 280 nm. UPLC-MS analysis after photoirradiation of peptide 1 in Ar-saturated solution for up to 9 h at 280 nm (using the integrating sphere) shows nearly exclusively the formation of product 7,

analyzed as 7-NEM, accompanied by a trace of 3-ox, analyzed as 3-NEM-ox (Figure S15A, Supporting Information). After 9 h of irradiation at 280 nm and derivatization of 7 into 7-NEM (because 1 and 7 are isobaric and not chromatographically

SCHEME 6: Reaction Scheme of the Formation of 9 during the UV Irradiation of an Aqueous Ar-Saturated Solution Containing Peptide 10 at pH 7.2**CHART 3: Representation of Products 9Ra and 9Rb Obtained after Photolysis at 253.7 nm of the Peptide (GGCRGGLLGRCGG) under a Continuous Stream of Ar, NEM Derivatization and Trypsin Digestion^a**^a The tryptic digestion sites are indicated through dashed lines.

separable), the ratio of **1/7** is estimated at 20%. For a more efficient and faster generation of **7**, peptide **1** was irradiated in a Pyrex tube in a Rayonet reactor equipped with a set of UV lamps, of which the spectral distribution is centered at 300 nm

and for which 93% of the photons emitted are in the wavelength range between 280 and 320 nm. The pyrex tube is opaque to wavelengths $\lambda < 280$ nm. Here, after 60 min of irradiation the ratio **1/7** reached 50% (Figure S15D, Supporting Information).

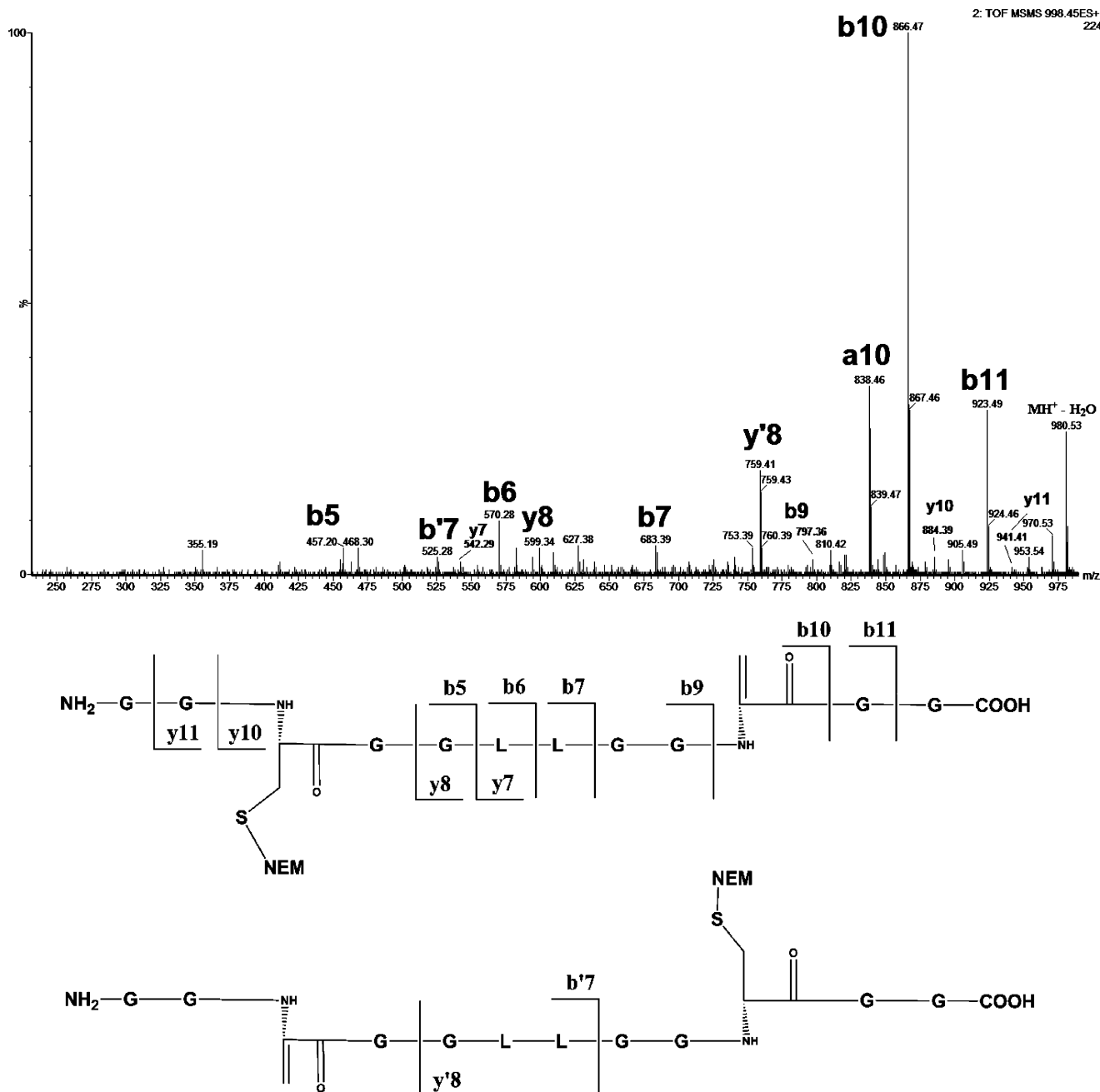


Figure 4. CID mass spectrum obtained on a Q-TOF mass spectrometer of product **12-NEM-C** and **12-NEM-N** (m/z 998.4) generated by UV irradiation at 253.7 nm of an Ar-saturated aqueous solution containing peptide **1**, followed by derivatization with NEM.

Importantly, for irradiation times >60 min the ratio **1/7** did not exceed 50%. This observation suggests that **1** and **7** may exist in some type of equilibrium.

We believe that the formation of secondary photoproducts, generated during the photodegradation of **1** at 253.7 nm, is due to the photolysis of the intermediate **7**. Unfortunately, product **7** is isobaric to **1** and not chromatographically separable from **1**. However, the possibility to derivatize the free thiol group present in **7** allowed to transform **7** into **7-NEM** which could be purified by HPLC and independently subjected to photoirradiation. The results on the photoirradiation of **7-NEM** are presented in section 3.1.7.

3.1.3. UV Irradiation of Peptide 1 under a Continuous Ar Flow. In section 3.1.1 we analyzed volatile mercaptans after transfer into a second vial through a continuous stream of Ar during UV photolysis; in contrast, section 3.1.2 summarizes our

product analysis of nonvolatile reaction products formed under stationary Ar saturation in the absence of a continuous Ar stream. Here, we have extended our product analysis to nonvolatile products generated under a continuous flow of Ar, i.e. conditions of section 3.1.1 (90 min of UV irradiation of a solution containing peptide **1**). Figure 3C,D reveals that under a continuous flow of Ar only product **9** (m/z 873.4, Scheme 5) is formed with a significant yield while peptide **1** is completely consumed (a trace of product **12-NEM-N/C** is visible in Figure 3D). These important differences to stationary Ar saturation (section 3.1.2) reveal that the removal of H₂S affects the formation of products **7**, **8**, and **10–12** (Schemes 4–7).

3.1.4. Quantification of Photoproducts of Peptide 1. (a) *Product Yields after 10 min of Irradiation at 253.7 nm.* The entire UPLC-MS chromatograms were integrated to compare the intensities of the photoproducts formed at pH 3.4 (Figure

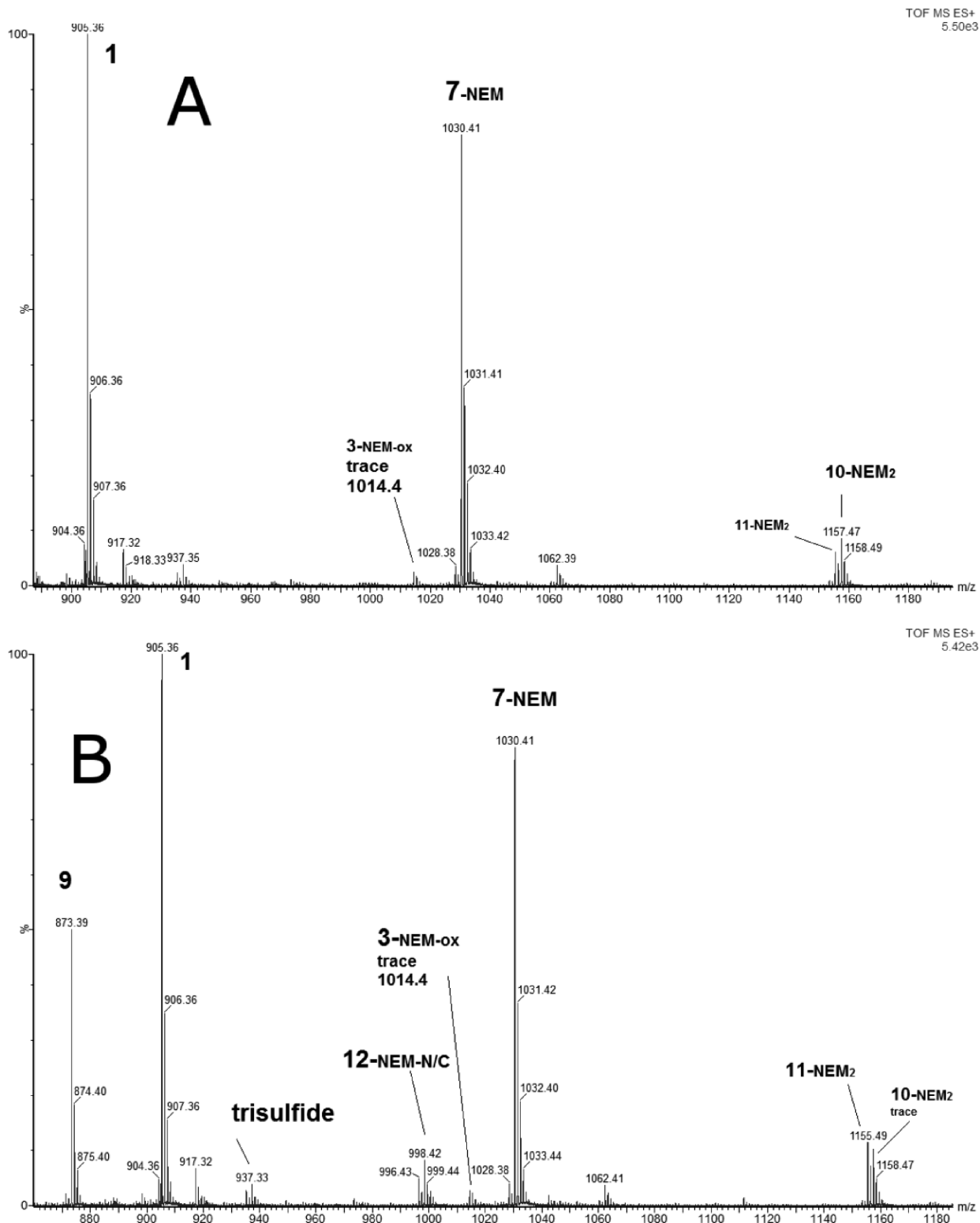


Figure 5. Integration of the overall chromatograms to compare the relative intensities of the products generated after UV irradiation at 253.7 nm of peptide 1 at pH 3.4 (A) and pH 7.2 (B).

5A) and 7.2 (Figure 5B). The integration consisted of a combination of the MS scans obtained from 8 to 22 min (Figure 3A,B). The peaks of the MS spectra generated after combination of the MS scans were smoothed and centered, and the intensities of the major peaks were added. Thus, the concentrations given in Table 1 were calculated based on the following assumption: the sum of the peak intensities of the remaining peptide 1 and the major photoproducts (7-NEM, 8, 9, 10-NEM₂, 11-NEM₂, 12-NEM-N/C) after irradiation must be equal to the intensities

of the peak of the native peptide prior to irradiation (400 μ M). The yields indicated in Table 1 correspond to the ratio:

$$\frac{[\text{product}]}{\sum [\text{products}] + [\text{native peptide}]} \times 100$$

Product yields depended on the applied dose but not on the dose rate, indicating that products were not the result of

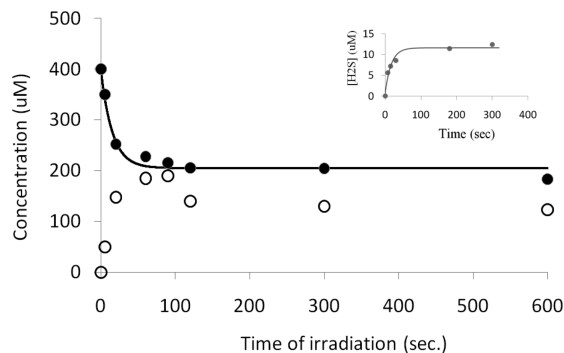


Figure 6. Time course of the evolution of photoproducts formed during UV irradiation ($\lambda = 253.7$ nm) of Ar-saturated aqueous solution containing peptide **1** at pH 3.5. Formation of product **7-NEM** (○) and degradation of peptide **1** (●). Inset: Time course of the formation of H_2S . After each time of photoirradiation, the solution was purged with Ar to transfer H_2S into a vial containing the fluorogenic reagent ThioGlo_1. The concentration of H_2S was deduced from a calibration curve of ThioGlo_1 solutions with different concentrations of Na_2S .

multiphotonic processes. However, several products resulted from secondary photolytic degradation of primary photoproducts (see also below).

(b) *Time-Dependent Change of 1,7-NEM and H_2S* . The evolution of the concentrations of **1**, **7-NEM** and H_2S was followed within the first minutes during UV irradiation ($\lambda = 253.7$ nm) of an Ar-saturated solution containing peptide **1** at pH 7.2 (Figure 6). We note that already after 2 min approximately equimolar concentrations of **1** and **7-NEM** are obtained (ca. $200 \mu M$ each). Parallel measurements of H_2S (Figure 6, inset) show that the rate of the photolytic degradation of **1** is equal to the initial rate of formation of H_2S (the initial concentration vs time profiles for H_2S formation and for the degradation of **1** can be fitted with first-order kinetics with $k = 0.6 s^{-1}$). This correlation implies that the photodegradation of **1** is rate-determining for H_2S formation. After 100 s, the formation of H_2S slows down significantly and the concentration of **7-NEM** decreases continuously by an amount of approximately $50 \mu M$ over the following 500 s while the concentration of **1** remains nearly constant. These observations suggest a complex mechanism for H_2S formation, which will be discussed below.

(c) *Photoirradiation in the Presence of CH_2Cl_2* . Peptide **1** was photoirradiated at 253.7 nm for 10 min in the presence and absence of an electron scavenger (CH_2Cl_2 , 10 mM) in Ar-saturated solutions at pH 7.2. The absolute peak intensities of the major photoproducts, measured by UPLC-MS analysis, are given in Table 3. The presence of an electron scavenger during the photolysis of peptide **1** does not modify the nature of the major photoproducts. However, the balance between these photoproducts is altered. For example, the presence of CH_2Cl_2 increases the yield of **8** by a factor >10 , while the yield of **9** is lowered by a factor >2 . The formation of product **7** is not affected by the presence of CH_2Cl_2 .

Based on the assumption that (i) the structures of **8** and **9** differ by the presence of a carbon–carbon double bond and (ii) H_2S originates from **7** (see Discussion), we can draw a relationship between the variations of the absolute intensities of the photoproducts as follows: the formation of **7** is not affected by the presence of an electron scavenger, suggesting that the formation of **7** does not involve any solvated electron (e_{aq}^-). In contrast, the large increase of **8** in the presence of CH_2Cl_2 , paralleled by a decrease of **9**, suggests that **8** can be reduced to **9** by e_{aq}^- . However, the fact that the presence of CH_2Cl_2 reduces the yield of product **9** by a factor 2 while that of **8** is enhanced >10 -fold suggests the existence of at least one alternative reaction pathway for the formation **9**, which does

TABLE 2: Relative Yields for the Formation of the Photoproducts Generated after Photolysis ($\lambda = 253.7$ nm) of Peptide **1 in Ar-Saturated Aqueous Solution at pH 3.4 and 7.2^a**

species	time of UV irradiation			
	10 min		2 min	
	pH 3.4	pH 7.2	pH 3.4	pH 7.2
1	58%	39%	63%	44%
	231 μM	156 μM	252 μM	176 μM
7-NEM	31%	31.5%	33%	35%
	123 μM	126 μM	132 μM	140 μM
9	trace	19.5%	trace	18%
		78 μM		72 μM
10-NEM₂	11%	trace	4%	trace
	46 μM		16 μM	
11-NEM₂	trace	3.5%	trace	3%
		14 μM		12 μM
12-NEM-N/C	trace	4.5%	trace	trace
		18 μM		

^a The concentrations are given with an uncertainty of $\pm 10\%$.

TABLE 3: Absolute Intensities of the Photoproducts Measured after UPLC-MS Analysis of an Irradiated Solution ($\lambda = 253.7$ nm) Containing Peptide **1 (400 μM) in the Presence and Absence of CH_2Cl_2 at pH 7.2**

product	without CH_2Cl_2	with CH_2Cl_2
7-NEM	10000	10120
8	65	765
9	7620	3010

not involve e_{aq}^- (see Discussion). A similar rationale applies to the yields of **13-N/C**.

3.1.5. Quantum Yield. Product **7** was obtained after 9 h of UV irradiation ($\lambda = 280$ nm, integrating sphere) of an Ar-saturated solution containing peptide **1** at pH 3.5. The quantum yield for the formation of **7** at 280 nm is equal to $\Phi = 0.09$.

3.1.6. NMR Analysis. The NMR spectra are presented in the Supporting Information (Figures S10–S13). The integrations of the NMR signals were normalized using the signal of the methyl groups of the leucine residues (chemical shift, δ^H 0.9).

(i) *NMR Analysis of Product 7-NEM.* Peptide **1** was irradiated in aqueous solution at 280 nm by means of the integrating sphere for up to 9 h at pH 3.5 in Ar-saturated solution. After 9 h of irradiation, an aliquot of the solution was derivatized with NEM at pH 7.5 for LC-MS analysis. Mass spectrometry confirmed the presence in the irradiated solution of only peptide **1** and the photoproduct **7-NEM**. Product **7-NEM** was purified by HPLC

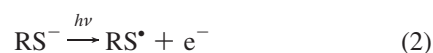
for ^1H -COSY measurements. After lyophilization, **7-NEM** was reconstituted in D_2O for NMR analysis. COSY NMR analysis of product **7-NEM** required 16 h of measurements in a solution with a pD about 2.4 (Figure S11, Supporting Information). Under such conditions, NEM will partially hydrolyze. Thus, to fully explain the proton coupling of the COSY NMR of product **7-NEM**, the hydrolysis of NEM has to be taken into account (Figure S11B, Supporting Information). The chemical shifts of the protons of the glycine and leucine residues and their connectivities in **7-NEM** are identical to those observed in peptide **1** (Figures S10 and S11, Supporting Information). Glycine residues display protons in the region $^1\text{H}\delta = 4.1$ – 4.08 ppm without any connectivity. Leucine residues are characterized by connectivities between $^1\text{H}\delta$ of γCH_3 and $^1\text{H}\delta$ of ^1CH ($^1\text{H}\delta = 0.9$ ppm coupling to $^1\text{H}\delta = 1.7$ ppm); between $^1\text{H}\delta$ of ^1CH and $^1\text{H}\delta$ of $^1\text{CH}_2$ ($^1\text{H}\delta = 1.7$ ppm coupling to $^1\text{H}\delta = 1.5$ ppm); and between $^1\text{H}\delta$ of $^1\text{CH}_2$ and $^1\text{H}\delta$ of ^1CH ($^1\text{H}\delta = 1.5$ ppm coupling to $^1\text{H}\delta = 4.2$, theory predicts a $^1\text{H}\delta$ for ^1CH of 4.5 ppm) (Figure S11A, Supporting Information). The connection between $^1\text{H}\delta$ of $^1\text{CH}_2$ ($^1\text{H}\delta = 3.2$ and 2.9 ppm) and $^1\text{H}\delta$ of ^1CH ($^1\text{H}\delta = 4.8$ ppm) of the cyclic-thioether is similar to the coupling observed in peptide **1** between the $^1\text{H}\delta$ of $^1\text{CH}_2$ and $^1\text{H}\delta$ of ^1CH groups of the cystine moiety (Figure S10, Supporting Information). In NEM, the protons of the ethyl group are connected through $^1\text{H}\delta(\text{CH}_2) = 4.0$ ppm and $^1\text{H}\delta(\text{CH}_3) = 1.2$ ppm (Figure S11, Supporting Information). These protons are observed at higher frequency when NEM is hydrolyzed (Figure S11B, Supporting Information). Indeed, theory predicts chemical shifts of $^1\text{H}\delta(\text{CH}_2) = 3.2$ ppm and $^1\text{H}\delta(\text{CH}_3) = 1.0$ ppm (Figure S11B, Supporting Information). The bond between sulfur and NEM in product **7-NEM** was already demonstrated by mass spectrometry. The ^1H -COSY NMR experiment confirms this bond. Indeed, the chemical shift $^1\text{H}\delta = 3.77$ or 3.8 ppm (depending on whether NEM is hydrolyzed or not) characterizes the proton in α -position to the sulfur atom. This latter proton ($^1\text{H}\delta = 3.77$ or 3.8 ppm) belongs to the original NEM moiety because the connectivity shows clearly that $^1\text{H}\delta = 3.77$ – 3.8 ppm couples with the two protons of the methylene group at $^1\text{H}\delta = 2.9$ ppm (or 2.7 ppm, if NEM is hydrolyzed) (Figure S11, Supporting Information). Theoretically, product **7-NEM** should display a $^1\text{H}\delta$ of ^1CH proton of the cyclic-thioether with an expected chemical shift around $^1\text{H}\delta = 4.4$ ppm, connected to the $^1\text{H}\delta$ of ^1CH group of the cyclic-thioether with an expected chemical shift of $^1\text{H}\delta = 5.1$ ppm. A comparison of the region of $^1\text{H}\delta = 4.4$ – 5.1 ppm of product **7-NEM** with that of the reference, peptide **1**, (Figure S12AB, Supporting Information), appears to indicate a connection between two protons with chemical shifts at $^1\text{H}\delta = 4.55$ and 4.81 ppm. These data need to be interpreted carefully due to the presence of the signal of HOD, which cannot be completely suppressed.

(ii) *NMR Analysis of Product 9.* Peptide **1** was photoirradiated either in H_2O or D_2O at 253.7 nm for up to 1 h under a continuous Ar stream. LC-MS analysis confirmed that peptide **1** was completely transformed into product **9** and that deuterons were incorporated into product **9** when photoirradiation was carried out in D_2O . Control experiments were performed where product **9** was produced in H_2O , isolated and redissolved in D_2O and then exposed to photoirradiation at $\lambda = 253.7$ nm for up to 45 min. Under these conditions no deuterons were incorporated into **9**, indicating that covalent H/D exchange must occur in a precursor/intermediate en route to **9**. The ^1H NMR spectra of product **9** and peptide **1** are similar (Figure S13A,B, Supporting Information). The chemical shifts of the protons of the leucine residues (CH_3 : $\delta^{\text{H}} = 0.9$ ppm; $^1\text{CH}_2$: $\delta^{\text{H}} = 1.75$ ppm; ^1CH : $\delta^{\text{H}} = 1.39$ ppm), and of the cysteine residues ($^1\text{CH}_2$: $\delta^{\text{H}} = 3.1$ – 3.3 ppm) do not show any significant modifications. However, we

note that in the region of the chemical shifts of the glycine residues ($^1\text{CH}_2$: $\delta^{\text{H}} = 3.9$ – 4.1 ppm) the δ^{H} at 3.9 ppm observed in peptide **1** is shifted toward higher frequency, $\delta^{\text{H}} = 3.75$ ppm, in product **9**. The integration of this signal ($\delta^{\text{H}} = 3.75$ ppm) yields two protons, consistent with this chemical shift representing one glycine residue. The shortening of the cycle in product **9**, due to the loss of a sulfur atom from peptide **1**, may modify the chemical shift of the protons of the glycine residues present between the cysteine residues. A signal with $\delta^{\text{H}} = 2.98$ ppm present only in the spectrum of product **9** might also be considered as a signal characteristic of product **9**. A connection between the protons of the $^1\text{CH}_2$ groups on both sides of the sulfur atom may rationalize this chemical shift. Indeed, in lanthionine, this region of chemical shift was assigned to such connection.^{57,58} When product **9** is generated in D_2O , LC-MS analysis indicated the covalent incorporation of about four deuteriums (Figure S13D, Supporting Information). The simulation is detailed in panels E and F. This deuterium incorporation is confirmed by ^1H NMR (Figure S13C, Supporting Information), where the signals of the cysteine $^1\text{CH}_2$ residues ($\delta^{\text{H}} = 3.1$ – 3.3 ppm) are absent (Figure S13C, Supporting Information), and the signals of the $^1\text{CH}_2$ protons of the glycine residues ($\delta^{\text{H}} 3.9$ – 4.3) are attenuated.

3.1.7. Photoirradiation of 7-NEM and 10. (i) *Photoproducts Generated after Photoirradiation of 7-NEM.* Product **7** was produced by photoirradiation of peptide **1** as described in section 3.1.2b. Product **7** was then derivatized with NEM. After HPLC purification of **7-NEM** (9% contamination by peptide **1**), the solution containing **7-NEM** was irradiated at 253.7 nm for 10 min at pH 7.2 (Figure 7). We note the formation of product **9** but no formation of H_2S and trisulfide. In addition to being photolabile, product **7-NEM** was also found to be heat-labile (see Supporting Information).

(ii) *Photoproducts Generated after Photoirradiation of 10.* Product **10** was produced by reduction of peptide **1** with DTT and purified by HPLC. [Peptide **10** was purified on a Zorbax Rx-C18 column ($15\text{ cm} \times 4.6\text{ mm}$), and eluted with a linear gradient delivered at a flow rate of 0.9 mL min^{-1} by a Varian 9012 pump system. The mobile phases consisted of water/acetonitrile/TFA at a ratio of 95%, 5%, and 0.1% (v:v:v) for solvent A and a ratio of 5%, 95%, and 0.1% (v:v:v) for solvent B. The following linear gradients were set: 5% of solvent B for 7 min, followed by 5–95% of solvent B within 11 min.] Peptide **10** was irradiated at 253.7 nm for 10 min in either H_2O or D_2O at pH/pD 7.2 and pH/pD 3.5 , respectively before derivatization with NEM. The results are presented in the Supporting Information, Figure S16. Peptide **10** is stable under UV irradiation at pH 3.5 (Figure S16A). Moreover, no photochemical deuterium incorporation was observed into **10-NEM**, suggesting that no sulfur radical is generated during UV irradiation at pH 3.5 (Figure S16A,C). In fact, at acidic pH, the protonation of the Cys residue in **10** prevents the formation of CysS $^{\bullet}$ through reaction 2. In contrast, for photoirradiation of peptide **10** at pH 7.2 , UPLC-MS analysis reveals the formation of three photoproducts: **1**, **9**, and **13-NEM-N/C** (Figure S16B). Importantly, photochemical deuterium incorporation is only detected for products **9** and **13-NEM-N/C** (Figure S16D,G). The native peptide **10** and peptide **1** do not show deuterium incorporation (Figure S16C,E)



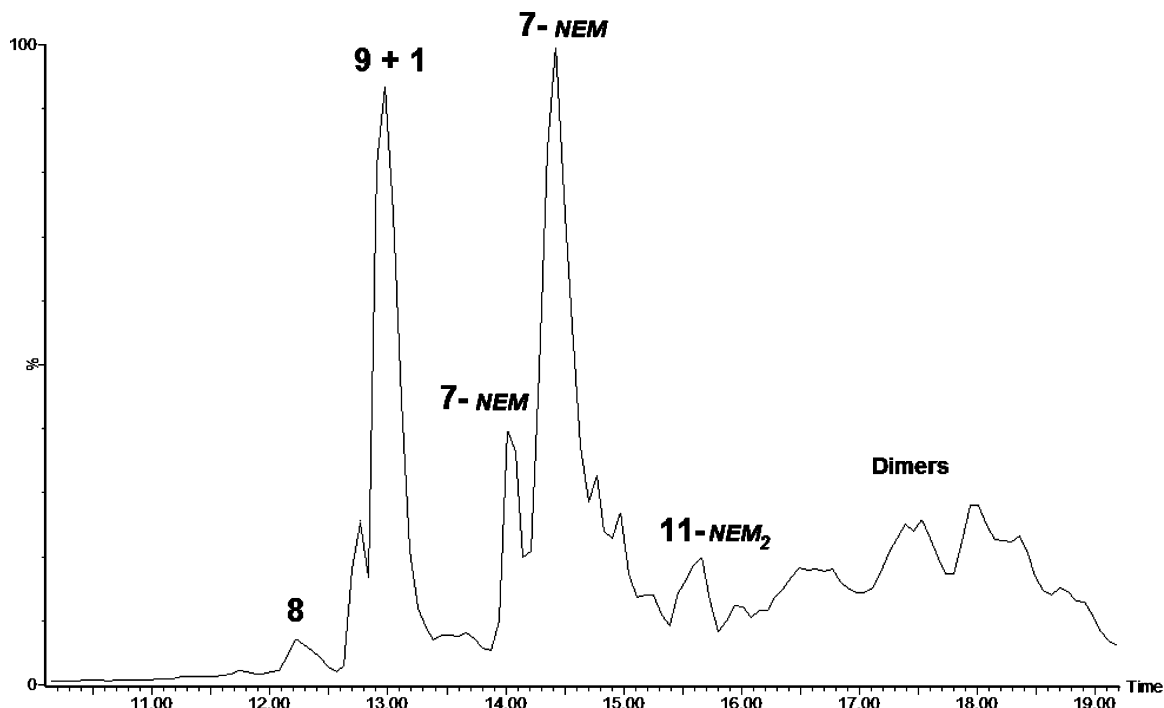
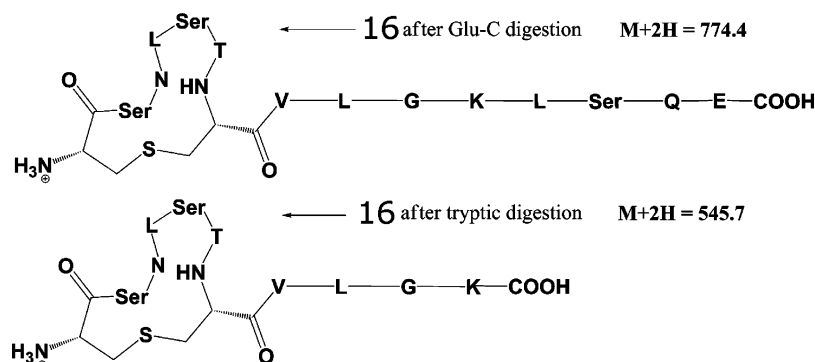


Figure 7. UPLC-MS analysis: formation of product **9** after photolysis at 253.7 nm of a solution containing the product **7-NEM**; x-axis, time; y-axis, relative abundance.

CHART 4: Photoproducts Obtained after UV Irradiation of sCT in Aqueous Solution^a



^a Photoproduct **16** is detected after either tryptic or Glu-C digestion. Only the serine residue is shown in three-letter code (Ser) in order to distinguish from a sulfur atom (S).

3.2. Analysis of the Photoproducts of sCT. sCT represents a 32-amino acid polypeptide with one intrachain disulfide bond between Cys1 and Cys7 (Chart 1). In the following, product analysis is focused only on a demonstration that products similar to those characterized for the model peptide **1** are also formed during the photolysis of this larger polypeptide. sCT was photoirradiated under an Ar atmosphere.

3.2.1. UV Irradiation of sCT at 253.7 nm at pH 6.2. (i) **Product 16.** sCT was photoirradiated for up to 10 min at 253.7 nm at pH 6.2 in Ar-saturated aqueous solution. After tryptic or Glu-C endoproteinase digestion, several peaks were chromatographically separated. Amid these, product **16** was identified through $m/z = 774.4$, $[M + 2H]^{+2}$, and $m/z = 545.7$, $[M + 2H]^{+2}$, after Glu-C or tryptic digestion, respectively (see Charts 1 and 4). The variation of mass between product **16** and the native peptide **15** is equal to 32 amu, suggesting the loss of one sulfur atom. This loss of 32 Da also suggests that **16** is structurally equivalent to **9** and may reveal cyclization between Cys1 and Cys7. Indeed, MS/MS fragmentation of the Glu-C fragment of product **16** clearly shows the fragments y3, y4, y6, y7-NH₃, and the fragments b6-NH₃ to b8-NH₃ (Figure S14,

Supporting Information). The absence of the remainder b and y fragments, involving the internal sequence CSNLSTC, suggests bond formation between Cys1 and Cys7 (Charts 1 and 4). Complementary MS/MS fragmentation of the tryptic fragment of product **16** leads to the same conclusion (data not shown). The addition of NEM in an attempt to derivatize any potential free thiol did not reveal any NEM modification of **16**, confirming the absence of a free thiol, which is consistent with the remaining sulfur being part of the cycle. Hence, the photolysis of sCT leads to a thioether linkage analogous to structure **9**.

3.2.2. Photolysis of sCT under Continuous Ar Flow. Analogous to product **9** from peptide **1**, we expect that continuous purging with Ar during the photolysis of sCT would not affect the formation of product **16**. Consistent with this expectation, the photolysis of sCT at 253.7 nm at pH 6.2 for up to 10 min under a continuous flow of Ar led to the formation of product **16**, analyzed by UPLC-MS (Figure 8). The peaks eluting with $t_R = 6.8, 8.1$, and 12.6 min represent expected masses of tryptic fragments of native sCT.

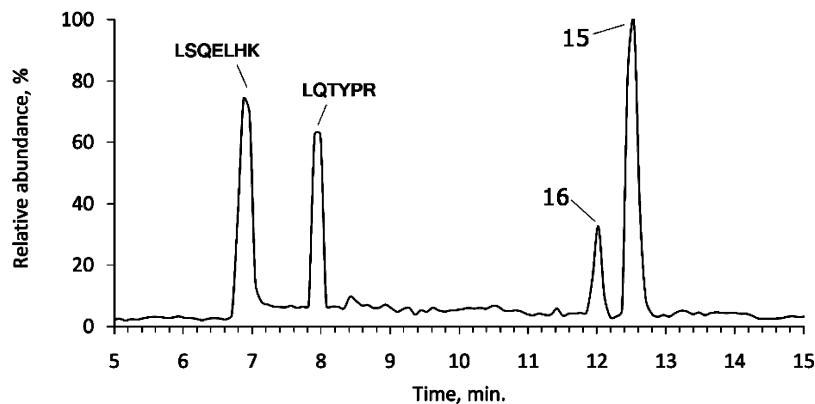


Figure 8. UPLC-MS trace obtained after tryptic digestion of a photoirradiated aqueous Ar-saturated solution of sCT. The Ar flow was maintained during the irradiation. The structures of peptides **15** and **16** are given in Charts 1 and 4, respectively.

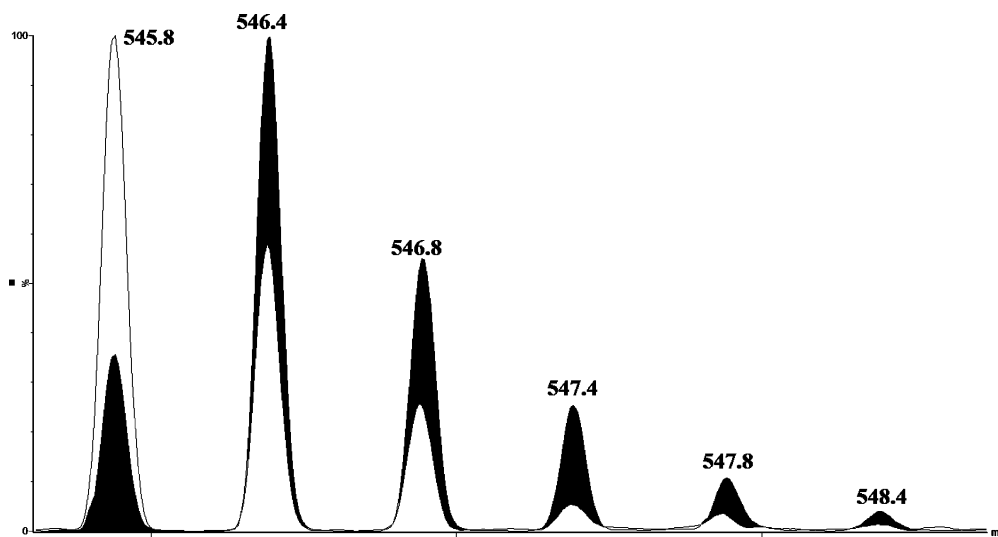


Figure 9. Variation of the percent base peak intensities (% Δ BPI) calculated after isotopic correction for the molecular ions (product **16**) obtained after UV irradiation of an aqueous Ar-saturated solution of sCT and digested with trypsin. Black areas represent the variation of the isotopic distribution obtained after MS analysis of **16** generated after UV irradiation of sCT in D₂O; x-axis, m/z ; y-axis, relative abundance in %.

3.2.3. H/D Exchange after Irradiation of sCT. Covalent H/D exchange was analyzed after tryptic digestion of photoirradiated Ar-saturated solutions of sCT in H₂O and D₂O. Product **16** shows significant deuterium incorporation with % Δ BPI = 65% for the incorporation of a single equivalent of D (Figure 9). Interestingly, the variation of the isotopic distribution after formation of **16** in D₂O solution is similar to that observed for product **9** in D₂O (Figure 6D). Control experiments reveal that the tryptic fragments of native sCT do not show deuterium incorporation.

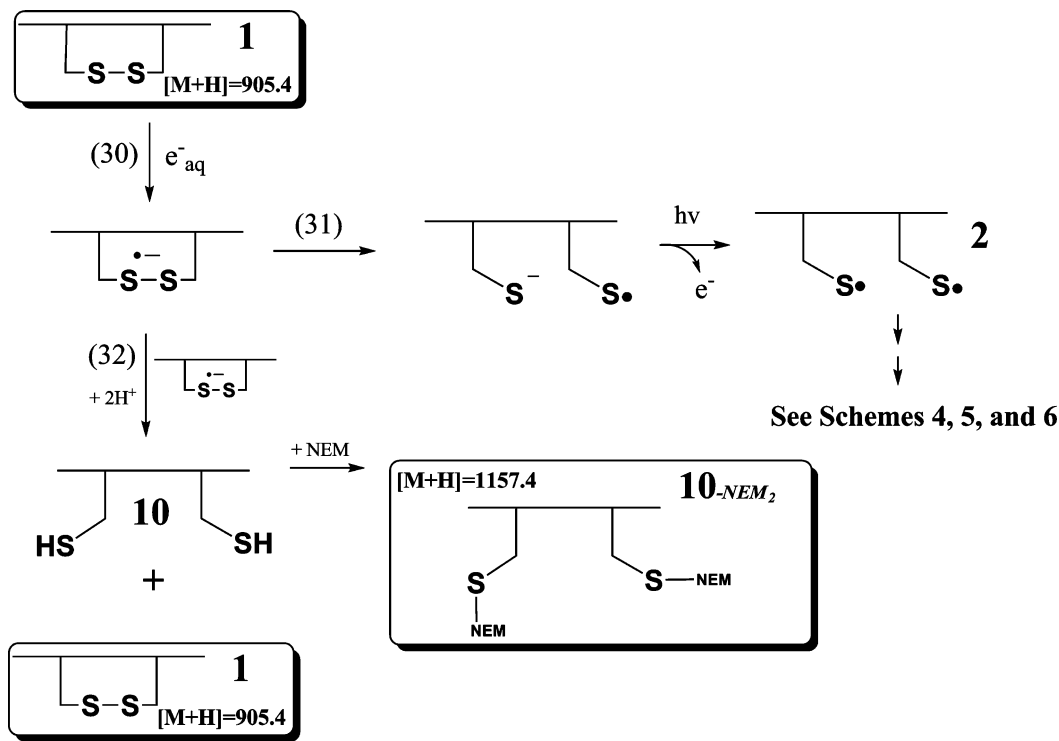
4. Discussion

4.1. Peptide 1. The photolysis of an intrachain disulfide bond in peptide **1** leads to a series of transient and stable products identified by MS/MS analysis. The nature of the stable products is consistent with the initial generation of CysS[•] radicals. The latter is not unexpected based on the broad absorption maximum of disulfides around 250 nm, which contains two transitions where the higher energy transition initially leads to a singlet radical pair of CysS[•].³⁹ Rapid intersystem crossing will efficiently generate a triplet radical pair of Cys[•].⁴⁸

When generated from an interchain disulfide, the CysS[•] radical pair ultimately generates a pair of disproportionation products

(thiol/thioaldehyde).^{37,59} Our present results demonstrate that such formal disproportionation products are most likely formed also after photodissociation of an intrachain disulfide bond but immediately react to form product **7**. Product **7** is sensitive to light (and heat) and serves as precursor for secondary photoproducts.

4.1.1. Formation of Product 7. The disproportionation of **2** leads to the formation of product **3** (Scheme 4, reaction 2), which is only detected as a trace after derivatization of its free thiol group with NEM and UPLC-MS analysis (products **3-NEM** and **3-NEM-ox**, where **3-NEM-ox** results from the hydrolysis of **3-NEM**, reactions 8 and 9). Interpretation of the MS scans (Figure 5) revealed that **3-NEM-ox** represents less than 5% of the total products. Interestingly, the MS/MS data on the NEM-labeled product **3-NEM-ox** indicate that **3** is the predominant stable disproportionation product, with a thioaldehyde function at the N-terminal Cys. The other isomer, with thioaldehyde at the C-terminal Cys and thiol at the N-terminal Cys was practically not observed, possibly due to rapid cyclization to product **7** (reaction 10), which can be derivatized with NEM to give **7-NEM**. The structure S–C–S in **7** displays some analogy to the S–C–S sequences present in 1,3,5-trithiane or 1,3-dithiane. The latter is characterized by an absorption spectrum

SCHEME 7: Reaction Scheme of the Formation of 10 during the Irradiation of an Aqueous Ar-Saturated Solution Containing Peptide 1 at pH 3.5


with a large shoulder at 250 nm.⁶⁰ Recent steady-state and laser flash photolysis studies of different 1,3,5-trithiane derivatives have demonstrated the formation of radical and/or ionic intermediates resulting from either homolytic or heterolytic cleavage of a C–S bond.^{61–64} These observations suggest that also the S–C–S entity in product **7** may be photosensitive at $\lambda = 253.7$ nm. Our experimental results clearly show that for $\lambda \geq 280$ nm the photolysis of **1** yields exclusively product **7**. The exposure of **7**-NEM to photoirradiation at $\lambda = 253.7$ nm leads to several photoproducts identical to those observed after direct photoirradiation of **1** at the same wavelength, and we expect analogous reactions for **7**. After 2 min of irradiation at 253.7 nm, approximately 50% of native peptide **1** is transformed into **7** (Figure 6). Beyond 2 min of irradiation, continuous photolysis leads to a faster degradation of **7** as compared to **1**. In Scheme 5, the photolytic decomposition of **7** is written as a diradical mechanism. However, an ionic intermediate (see inset), would account for similar products.

4.1.2. Formation of Product 10. Product **10** (observed as **10**-NEM₂ after derivatization with NEM) is formed predominantly at acidic pH (Figure 3B). This pH dependency most likely reflects a subsequent pH-dependent photodegradation of **10**, which is more efficient at neutral pH. In fact, we observed that peptide **10** is stable toward photodegradation ($\lambda = 253.7$ nm) at acidic pH (Figure S16A, Supporting Information) while photoirradiation at neutral pH led to the formation of peptide **1** and products **9** and **13**-N/C (Figure S16B, Supporting Information). Hence, we conclude that secondary photoproducts originating from the photolysis of **10** contribute to overall product formation during the photolysis of peptide **1** at neutral pH (Scheme 6).

At present we believe that product **10** originates from the reduction of **1** (Scheme 7), where the solvated electron (Scheme 7, reaction 30) is provided most likely by the established photolysis of HS^{–65} (or of other deprotonated thiols). Such mechanism would be consistent with the absence of **10** under

conditions of constant removal of H₂S through a continuous stream of Ar.

4.1.3. Formation of Product 9 and H₂S. Product **9** and H₂S are observed at neutral pH (stationary Ar saturation). Mechanistically, they form through further reaction of **7** and/or the photolysis of **10** at neutral pH.

4.1.3.1. Photolysis of Product 7. By analogy to the photochemistry of 1,3,5-trithiane, the photolysis of **7** is expected to lead to the homolytic/heterolytic cleavage of either of the two C–S bonds. The cleavage at site (a) (Scheme 5, reaction 14) is accompanied by the formation of either radical **14a** and HS[•] or carbocation and HS[–] (see “ionic intermediate”). In both cases, the intermediates should convert into **8** and H₂S (Scheme 5, reaction 15). HS[•] can abstract a hydrogen atom according to reaction 15, leading to product **8** and H₂S. Readdition of H₂S to **8** would regenerate **7** (Scheme 5, reaction 16). However, at pH 7.2, H₂S is partially deprotonated (HS[–]) and subject to photolysis yielding solvated electrons (eq 2). Hydrated electrons are likely the source of reduction of **8** to **9** (Scheme 5, reaction 17), consistent with the effect of added CH₂Cl₂ as an electron scavenger (see Table 3). The question is whether solvated electrons react directly with **8** or reduce **1** to the radical anion (Scheme 7, reaction 30), where the radical anion of **1** further reduces **8**. The latter appears more probable based on the fast reaction of solvated electrons with organic disulfides^{25,26} and the concentration ratio, where $[1] > [8]$. Additional sources of solvated electrons are the photolysis of **10**, **11**, and even **7** (if deprotonated). If solvated electrons are involved in the reduction of **8** (Scheme 5, reaction 17), it is reasonable to invoke an intermediate radical anion (Scheme 7, reaction 30). We have to take into account that this radical anion may be a source of **2** and, consequently, lead to the formation of the photoproducts described in Schemes 4, 5, and 6. In addition, the disproportionation of two radical anions would lead to the formation of **10** and **1** (Scheme 7, reaction 32).

4.1.3.2. Photolysis of Product 10. (i) *In H₂O.* The thiol groups of product **10** are in equilibrium with thiolate groups, which are expected to convert into thiyl radicals under UV irradiation at neutral pH (**10a**N/C, Scheme 6, reactions 18). In principle, such thiyl radical can abstract a hydrogen atom from any of the $^{\alpha}\text{C}$ –H bonds including that of the second Cys residue. The latter process would generate the $^{\alpha}\text{C}$ -centered radicals, **10b**N/C (Scheme 6, reactions 19), which can undergo β -elimination (reactions 20–21) to form products **12**-N/C, which are detected as **12**-NEM-N/C after derivatization with NEM (Figures 3A and 7B). Cyclization of **12**-N/C generates **9** (reaction 23). We note that the photolysis of **10** would also generate an intermediary disulfide radical anion identical to that generated through the one-electron reduction of **1**. In fact, one-electron reduction of **1** was suggested as a mechanism leading to the formation of **10**. We, therefore, suggest that any peptide **12**-N/C generated through the photolysis of **1** is likely the result of branching of the disulfide radical anion toward the formation of **10a**N/C and **10b**N/C rather than the formation of **10** followed by photolysis of **10**.

(ii) *In D₂O.* Peptide **10** was irradiated in H₂O and D₂O at acidic pH (Figure S16A, Supporting Information). No photo-degradation was observed, i.e. after NEM derivatization, we only detected the presence of **10**-NEM₂. In addition, no deuterium incorporation was observed. This result demonstrates that peptide **10** is not photosensitive at acidic pH. In contrast, the observation of covalent deuterium incorporation into **9** and **13**-NEM-N/C during the photolysis of **10** at neutral pH demonstrates the existence of intramolecular H-atom transfer involving Cys* (Figure S16B,D,G, Supporting Information). ¹H NMR of product **9** generated in D₂O clearly demonstrates that covalent deuterium incorporation occurs at the βC -atoms of the cysteine residues (Figure S13C, the signals of βCH_2 cysteine are absent (Supporting Information)). This pattern of deuterium incorporation is consistent with the intermediacy of radicals **10a**N/C and **10b**N/C. For example, through a reversible 1,2-H-shift in **10a**N (cf. Scheme 2, reactions 1e and 1f), deuterium incorporation would occur at βC of the N-terminal Cys thiyl radical. Through H-transfer from the C-terminal Cys mercapto group, a thiyl radical would form on the C-terminal Cys residue (**10a**C). This thiyl radical would, again, be subject to reversible 1,2-H-shift, which would lead to deuterium incorporation on the βC atom of the C-terminal Cys residue. A single H-transfer from the $^{\alpha}\text{C}$ –H group to the Cys thiyl radical (cf. Scheme 6, reactions 19) could trigger β -elimination of HS* (equilibrium 21) to yield products **12**-N/C, followed by either cyclization (to product **9**) or reduction (to products **13**-N/C).

4.1.3.3. Product Formation under Continuous Ar Flow. Under a continuous flow of Ar, H₂S is efficiently removed from the solution. These conditions prevent the readdition of H₂S to product **8** and therefore the regeneration of **7** (Scheme 5). Interestingly, under such conditions we did not observe the formation of **8** but only product **9** (Figure 3D). As H₂S/HS[−] cannot be a source of solvated electrons under a continuous Ar flow, we suggest that the deprotonated forms of **7** and of the other thiols generated during the photolysis of **1** are the source of e_{aq}^{-} .

The photolytic formation of **9** in D₂O revealed covalent deuterium incorporation. This observation was demonstrated by LC-MS and ¹H NMR analysis. LC-MS analysis allowed to estimate the number of deuterium incorporated into each molecule of **9** between 2 and 4 deuterons. ¹H NMR analysis clearly demonstrates that deuterium incorporation occurs at the βC position of the cysteine residues. This can be rationalized,

by a reduction of the carbon–carbon double bond of product **8**. In D₂O the reduction of **8** into **9** would lead to the incorporation of two deuterons into the $^{\alpha}\text{C}$ and βC positions of the cysteine residue. However, this reaction cannot fully explain the ¹H NMR data (Figure S13C, Supporting Information), which demonstrate the entire absence of βC –H protons in **9**. We observed that the number of deuterium incorporated into **9** is dependent on the time of photoirradiation. Indeed, the number of deuterium incorporated into **9** calculated after 10 min of photoirradiation of either peptide **1** or **10** is equal to 2 (Figure S16D, Supporting Information) whereas, after 1 h of photoirradiation the number of deuterium incorporated is equal to 4 (Figure S13D, Supporting Information). To explain the full transformation of the βCH_2 group into βCD_2 in **9** and the time dependency we suggest the involvement of equilibria 24 and 25 (Scheme 5), i.e., photolytic cleavage of the C–S bond of the thioether of **7**. In D₂O, H₂S is in equilibrium with D₂S, and may add on the carbon–carbon double bond of **8** to regenerate intermediate **7** through reaction 16 leading to the incorporation of deuterium into **7** (Scheme 5). To explain the deuterium incorporation into the second βCH_2 group, we suggest that after the cleavage at site (b) (Scheme 5, 24) of the C–S bond of **7**, the intermediate **14b** undergoes a reversible 1,2-H-shift which would lead to deuterium incorporation into both βC carbons of the cysteine residues. The recombination of the radicals in **14b** to regenerate **7** is probably the most favorable process. Thus, the unfavorable equilibrium 24 toward the formation of **14b** may explain why the deuterium incorporation into **9** is time dependent.

4.1.4. Formation of Product 11. The photolysis of **7** ($\lambda < 280$ nm) can lead to the cleavage of the second C–S bond. This cleavage indicated through (b) in Scheme 5 gives rise to the intermediate **14b** (Scheme 5, reaction 24). At present, we do not see any other possibility for the formation of **11** (observed as **11**-NEM₂) than a 1,2-H-shift (reaction 25). A 1,2-H-shift would convert **14b** into **14c** (Scheme 5, reaction 25). Theoretical calculations of such 1,2-H-shift reaction of a thiyl radical (of 2-mercaptoethanol) show that the equilibrium between thiyl radical and C-centered radical lies more or less fully on the side of the thiyl radical.^{66,67} Nevertheless, a rate constant of $k_{1,2\text{-H-shift}} \approx 10^3 \text{ s}^{-1}$ (at 20 °C) was reported.⁶⁶ Potentially, even small amounts of the βC^{\bullet} radical efficiently remove **14b** from equilibrium 25 via reaction 26. Hence, specifically the formation of **11** supports the occurrence of 1,2-H-shift processes. When the photolysis of peptide **1** was carried out under an Ar stream, we did not observe the formation of **11**. We suggest that the removal of H₂S favors reactions 14–17. An efficient 1,2-H-shift as discussed above would also open the possibility for the formation of **7** from **2** via equilibria 28 and 24 (Scheme 5).

4.2. sCT. sCT was used as a model to extend our mechanistic studies to an intrachain disulfide bond in a larger polypeptide. A variety of photoproducts was generated in the presence of Ar, of which only product **16** is important for the present paper. Based on the reaction mechanisms proposed for the intrachain disulfide bond in model peptide **1** (Schemes 4–7), we assume that elimination of HS* precedes the formation of **16**. The UPLC-MS analysis of an irradiated Ar-saturated solution of sCT, continuously flushed with Ar, shows results analogous to those obtained after irradiation of peptide **1** under similar conditions. Only one photoproduct could be readily observed after digestion of irradiated sCT with trypsin (Figure 8). This unique product could be assigned to the structure of **16** (Chart 4) which is equivalent to the structure of **9** observed after irradiation of **1** under similar conditions. Thus, an identical mechanism appears

to operate after disulfide photolysis of **1** and sCT. We note that the deuterium incorporation observed in product **16** is similar to that observed in product **9**. The similarity of the covalent H/D exchange (Figure S16D (Supporting Information) versus Figure 9) in both products is one additional evidence that **16** is formed through an identical process as detailed above for the formation of **9**.

4.3. Thiyl Radicals vs Perthiyl Radicals. We have limited our mechanistic considerations to the reactions of thiyl radicals since previous articles specifically reported on the predominant generation of thiyl radicals during the photolysis of peptide disulfide bonds.^{5,47} It is important, however, to discuss any potential role of perthiyl radicals in product formation. Product **7** contains two sulfur atoms but not a sulfur–sulfur bond, which is consistent with thiyl radicals (and not a perthiyl radical) as precursor for product **7**. A similar consideration applies to products **10** and **11**. On the other hand, product **12** could form via initial photolytic C–S bond cleavage, followed by disproportionation,⁴⁴ and reduction of an intermediary perthiol to thiol. Subsequent cyclization would then yield product **9**. This process would, however, fail to rationalize the extent of covalent H/D exchange at the Cys β C positions of product **9** observed for reactions performed in D₂O, which we suggest to involve reversible 1,2-H-shifts of thiyl radicals (with a reported rate constant for the 1,2-H-shift of thiyl radicals of $k \approx 10^3 \text{ s}^{-1}$ at $T = 20^\circ \text{C}$ ⁶⁶). For perthiyl radicals, covalent H/D exchange at the Cys β C atom would require a 1,3-H-shift (and based on calculations for intramolecular H-atom transfer reactions in aliphatic carbon-centered radicals the activation energies for 1,2- and 1,3-H-shifts are comparable⁶⁸). However, hydrogen abstraction by perthiyl radicals is significantly slower compared to that of thiyl radicals.⁶⁹ Importantly, the formation of **9** via perthiyl radicals would leave at least one Cys β C–H bond intact (i.e., no covalent H/D exchange at the carbon-centered radical which would form through the initial C–S bond cleavage yielding the perthiyl radical), which is in contrast to our experimental NMR data.

5. Conclusion

The photolysis of an intrachain disulfide yields a cyclic dithiohemiacetal **7**, which is isobaric to the disulfide bond. This primary photoproduct, which is characteristic for an intrachain disulfide bond peptide, is involved in secondary photoreactions, which generate, among others, a cyclic-thioether peptide (product **9**) containing the structure of lanthionine, and H₂S. The photoirradiation of an interchain disulfide bond leads to disproportionation products of the cysteinyl radicals (thiol and thioaldehyde). However, contrary to intrachain disulfide bond, these two functions are held by two different strands after the photoirradiation rendering the readdition of the thiol group onto the thioaldehyde less probable. The use of UV light in the production of proteins in the biotechnology industry may lead to the generation of such photoproducts. Early on, small levels of lanthionine had been shown to be formed upon photolysis of isolated cystine;⁷⁰ however under our reaction conditions product **9** and **16** were major products. Importantly, cyclic thioethers analogous to **9** and **16** have been isolated after the production of human growth hormone⁵⁶ and in an antibody.⁷¹ While the formation of such products has traditionally been explained via thiol reaction with dehydroalanine, we have now also to consider the photolytic degradation of disulfide as a potential source.

Acknowledgment. We are grateful to Amgen Inc. for financial support. We thank Dr. Justin Douglas for technical

and theoretical assistance in the acquisition and interpretation of the NMR data.

Supporting Information Available: Chart S1 and Figures S1–S16 are available. This material is available free of charge via the Internet at <http://pubs.acs.org>.

References and Notes

- (1) Volkin, D. B.; Mach, H.; Middaugh, C. R. *Mol. Biotechnol.* **1997**, *8*, 105.
- (2) Ellison, D.; Stalteri, M. A.; Mather, S. J. *Biotechniques* **2000**, *28*, 318.
- (3) Lam, X. M.; Yang, J. Y.; Cleland, J. L. *J. Pharm. Sci.* **1997**, *86*, 1250.
- (4) Creed, D. *Photochem. Photobiol.* **1984**, *39*, 577.
- (5) Everett, S. A.; Schöneich, C.; Stewart, J. H.; Asmus, K. D. *J. Phys. Chem.* **1992**, *96*, 306.
- (6) Wang, W.; Singh, S.; Zeng, D. L.; King, K.; Nema, S. *J. Pharm. Sci.* **2007**, *96*, 1.
- (7) Cordoba, A. J.; Shyong, B. J.; Breen, D.; Harris, R. J. *J. Chromatogr. B Anal. Technol. Biomed. Life Sci.* **2005**, *818*, 115.
- (8) Gaza-Bulseco, G.; Liu, H. *Pharm. Res.* **2008**, *25*, 1881.
- (9) Stubbe, J.; van Der Donk, W. A. *Chem. Rev.* **1998**, *98*, 705.
- (10) Chatgililoglu, C.; Asmus, K.-D. *Sulfur-centered reactive intermediates in chemistry and biology*; Plenum Press: New York, 1991; Vol. 197; NATO ASI Series. Life Sciences.
- (11) Wardman, P. *J. Phys. Chem. Ref. Data* **1989**, *18*, 1637.
- (12) Ferreri, C.; Costantino, C.; Landi, L.; Mulazzani, Q.; Chatgililoglu, C. *Chem. Commun. (Camb.)* **1999**, 407.
- (13) Tamba, M.; O'Neil, P. J. *Chem. Soc., Perkin Trans.* **1991**, *2*, 1681.
- (14) Sprinz, H.; Adhikari, S.; Brede, O. *Adv. Colloid Interface Sci.* **2001**, *89–90*, 313.
- (15) Sprinz, H.; Schwinn, J.; Naumov, S.; Brede, O. *Biochim. Biophys. Acta* **2000**, *1483*, 91.
- (16) Akhlag, M. S.; Schuchmann, H. P.; von Sonntag, C. *Int. J. Radiat. Biol.* **1987**, *51*, 91.
- (17) Pogocki, D.; Schöneich, C. *Free Radical Biol. Med.* **2001**, *31*, 98.
- (18) Schöneich, C.; Asmus, K. *Radiat. Environ. Biophys.* **1990**, *29*, 263.
- (19) Schöneich, C.; Bonifačić, M.; Asmus, K. *Free Radical Res. Commun.* **1989**, *6*, 393.
- (20) Schöneich, C.; Dillinger, U.; von Bruchhausen, F.; Asmus, K. *Arch. Biochem. Biophys.* **1992**, *292*, 456.
- (21) Barron, L. B.; Waterman, K. C.; Filipiak, P.; Hug, G. L.; Nauser, T.; Schöneich, C. *J. Phys. Chem. A* **2004**, *108*, 2247.
- (22) Bonifačić, M.; Asmus, K. D. *J. Phys. Chem.* **1976**, *80*, 2426.
- (23) Bonifačić, M.; Asmus, K. D. *Int. J. Radiat. Biol.* **1984**, *46*, 35.
- (24) Bonifačić, M.; Schaefer, K.; Moeckel, H.; Asmus, K. D. *J. Phys. Chem.* **1975**, *79*, 1496.
- (25) Purdie, J.; Gillis, H.; Klassen, N. *Can. J. Chem.* **1973**, *51*.
- (26) Hoffman, M. Z.; Hayon, E. *J. Am. Chem. Soc.* **1972**, *94*, 7950.
- (27) Neves-Petersen, M. T.; Gryczynski, Z.; Lakowicz, J.; Fojan, P.; Pedersen, S.; Petersen, E.; Petersen, B. S. *Protein Sci.* **2002**, *11*, 588.
- (28) Prompers, J. J.; Hilbers, C. W.; Pepermans, H. A. *FEBS Lett.* **1999**, *456*, 409.
- (29) Miller, B. L.; Hageman, M. J.; Thamann, T. J.; Barron, L. B.; Schöneich, C. *J. Pharm. Sci.* **2003**, *92*, 1698.
- (30) Vanhooren, A.; De Vriendt, K.; Devreese, B.; Chedad, A.; Sterling, A.; Van Dael, H.; Van Beeumen, J.; Hanssens, I. *Biochemistry* **2006**, *45*, 2085.
- (31) Vanhooren, A.; Devreese, B.; Vanhee, K.; Van Beeumen, J.; Hanssens, I. *Biochemistry* **2002**, *41*, 11035.
- (32) Mozziconacci, O.; Williams, T.; Kerwin, B.; Schöneich, C. *J. Phys. Chem. B* **2008**, *112*, 15921.
- (33) Rauk, A.; Yu, D.; Taylor, J.; Shustov, G. V.; Block, D. A.; Armstrong, D. A. *Biochemistry* **1999**, *38*, 9089.
- (34) Nauser, T.; Casi, G.; Koppenol, W.; Schöneich, C. *J. Phys. Chem. B* **2008**, *112*, 15034.
- (35) Rauk, A.; Yu, D.; Armstrong, D. A. *J. Am. Chem. Soc.* **1998**, *120*, 8848.
- (36) Rauk, A.; Armstrong, D. A.; Fairlie, D. P. *J. Am. Chem. Soc.* **2000**, *122*, 9761.
- (37) Mozziconacci, O.; Sharov, V.; Williams, T. D.; Kerwin, B. A.; Schöneich, C. *J. Phys. Chem. B* **2008**, *112*, 9250.
- (38) Nauser, T.; Casi, G.; Koppenol, W.; Schöneich, C. *Chem. Commun.* **2005**, 3400.
- (39) Thompson, S. D.; Carroll, D. G.; Watson, F.; O'Donnell, M.; McGlynn, S. P. *J. Chem. Phys.* **1966**, *45*, 1367.
- (40) Rinker, A.; Halleman, C. D.; Wedlock, M. R. *Chem. Phys. Lett.* **2005**, *414*, 505.
- (41) Smismán, E. E.; Sorenson, J. R. *J. Org. Chem.* **1965**, *30*, 4008.
- (42) Joshi, A.; Yang, G. C. *J. Org. Chem.* **1981**, *46*, 3736.

- (43) Hawari, J. A.; Griller, D.; Lossing, F. P. *J. Am. Chem. Soc.* **1986**, *108*, 3273.
- (44) Rosenfeld, S. M.; Lawler, R. G.; Ward, H. R. *J. Am. Chem. Soc.* **1972**, *94*, 9255.
- (45) Morine, G.; Kuntz, R. *Photochem. Photobiol.* **1981**, *33*, 1.
- (46) Burkey, T. J.; Hawari, J. A.; Lossing, F. P.; Luszyk, J.; Sutcliffe, R.; Griller, D. *J. Org. Chem.* **1985**, *50*, 4966.
- (47) Kolano, C.; Helbing, J.; Bucher, G.; Sander, W.; Hamm, P. *J. Phys. Chem. B* **2007**, *111*, 11297.
- (48) Autrey, T.; Devadoss, C.; Sauerwein, B.; Franz, J. A.; Schuster, G. B. *J. Phys. Chem.* **1995**, *99*, 869.
- (49) Abe, K.; Kimura, H. *J. Neurosci.* **1996**, *16*, 1066.
- (50) Kamoun, P. *Amino Acids* **2004**, *26*, 243.
- (51) Li, L.; Bhatia, M.; Moore, P. K. *Curr. Opin. Pharmacol.* **2006**, *6*, 125.
- (52) Ishigami, M.; Hiraki, K.; Umemura, K.; Ogasawara, Y.; Ishii, K.; Kimura, H. *Antioxid. Redox Signaling* **2009**, *11*, 205.
- (53) Wright, S. K.; Viola, R. E. *Anal. Biochem.* **1998**, *265*, 8.
- (54) Storey, B. T.; Alvarez, J. G.; Thompson, K. A. *Mol. Reprod. Dev.* **1998**, *49*, 400.
- (55) Serjeant, E.; Dempsey, B. *Ionization constants of Inorganic Acids and Bases in Aqueous Solution*, 2nd ed.; Perrin, D. D., Ed.; Pergamon: Oxford, UK, 1982; IUPAC Chemical Data Series, No. 29.
- (56) Datola, A.; Richert, S.; Bierau, H.; Agugiaro, D.; Izzo, A.; Rossi, M.; Cregut, D.; Diemer, H.; Schaeffer, C.; Van Dorselaer, A.; Giartosio, C. E.; Jone, C. *ChemMedChem* **2007**, *2*, 1181.
- (57) Mustapa, M. F. M.; Harris, R.; Mould, J.; Chubb, N. A. L.; Schultz, D.; Driscoll, P. C.; Tabor, A. B. *Tetrahedron Lett.* **2002**, *43*, 8359.
- (58) Zhou, H.; van der Donk, W. A. *Org. Lett.* **2002**, *4*, 1335.
- (59) Fung, Y. M.; Kjeldsen, F.; Silivra, O. A.; Chan, T. W.; Zubarev, R. A. *Angew. Chem., Int. Ed. Engl.* **2005**, *44*, 6399.
- (60) Bergson, G.; Claeson, G.; Schotte, L. *Acta Chem. Scand.* **1962**, *16*, 1159.
- (61) Hug, G. L.; Janeba-Bartoszewicz, E.; Filipiak, P.; Pedzinski, T.; Kozubek, H.; Marciniak, B. *Pol. J. Chem.* **2008**, *82*, 883.
- (62) Janeba-Bartoszewicz, E.; Hug, G. L.; Andrzejewska, E.; Marciniak, B. *J. Photochem. Photobiol. A* **2006**, *177*, 17.
- (63) Burdzinski, G.; Marciniak, B. *Chem. Phys. Lett.* **2008**, *465*, 45.
- (64) Asmus, K. D.; Hug, G. L.; Bobrowski, K.; Mulazzani, Q. G.; Marciniak, B. *J. Phys. Chem. A* **2006**, *110*, 9292.
- (65) Das, T. N.; Huie, R. E.; Neta, P.; Padmaja, S. *J. Phys. Chem. A* **1999**, *103*, 5221.
- (66) Zhang, X.; Zhang, N.; Schuchmann, H.-P.; von Sonntag, C. *J. Phys. Chem.* **1994**, *98*, 6541.
- (67) Naumov, S.; Von Sonntag, C. *J. Phys. Org. Chem.* **2005**, *18*, 586.
- (68) Viscolcz, B.; Lendvay, G.; Körtvélyesi, T.; Seres, L. *J. Am. Chem. Soc.* **1996**, *118*, 3006.
- (69) Everett, S. A.; Folkes, L. K.; Wardman, P.; Asmus, K. D. *Free Radical Res.* **1994**, *20*, 387.
- (70) Forbes, W.; Savige, W. *Photochem. Photobiol.* **1962**, *1*, 1.
- (71) Tous, G. I.; Wei, Z.; Feng, J.; Bilbulian, S.; Bowen, S.; Smith, J.; Strouse, R.; McGeehan, P.; Casas-Finet, J.; Schenerman, M. A. *Anal. Chem.* **2005**, *77*, 2675.

JP910789X